

N78-28585

Multispectral Data Restoration Study

Final Report

BSR 4246

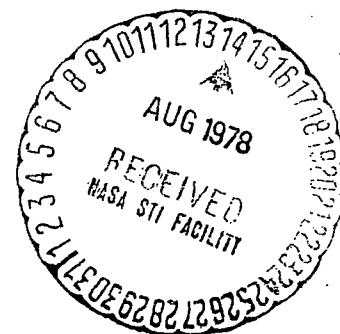
May 1977

Dr. Navinchandra J. Shah & Mr. C.L. Wilson  
Bendix Aerospace Systems Division  
3621 S. State Road  
Ann Arbor, Michigan 48107

Prepared for:

Goddard Space Flight Center  
Greenbelt, Maryland 20771

Contract No. NAS5-23384



TECHNICAL REPORT STANDARD TITLE PAGE

1. Report No.		2. Government Accession No.		3. Recipient's Catalog No.	
4. Title and Subtitle Multispectral Data Restoration Study				5. Report Date May 1977	
				6. Performing Organization Code	
7. Author(s) Dr. Navinchandra J. Shah & Mr. C.L. Wilson				8. Performing Organization Report No. BSR 4246	
9. Performing Organization Name and Address Bendix Aerospace Systems Division 3621 S. State Road Ann Arbor, Mich. 48107				10. Work Unit No.	
				11. Contract or Grant No. NAS5-23384	
12. Sponsoring Agency Name and Address Goddard Space Flight Center Greenbelt, Maryland 20771				13. Type of Report and Period Covered Final Report	
				14. Sponsoring Agency Code	
15. Supplementary Notes					
16. Abstract  The results from this study reveal that: (1) Bendix Restoration is superior to cubic convolution as a resampling technique; (2) it appears that Bendix restored data can also be made superior to the original data; (3) optimization of spatial and radiometric characteristics cannot be determined from presently available results; and (4) promising results from Bendix Restoration require further investigation to study tradeoffs between sampling interval and radiometric accuracy, and the effect of assumed signal to noise ratio on the restored data.					
17. Key Words (Selected by Author(s))  Restoration and Resampling				18. Distribution Statement	
19. Security Classif. (of this report) Unclassified		20. Security Classif. (of this page) Unclassified		21. No. of Pages	22. Price*

## CONTENTS

	<u>Page</u>
1. INTRODUCTION AND SUMMARY	1-1
1.1 BACKGROUND	1-1
1.2 PROJECT OBJECTIVE	1-3
1.3 SUMMARY OF RESULTS	1-4
2. PROJECT OBJECTIVE AND SCOPE OF EFFORT	2-1
2.1 PROJECT OBJECTIVE	2-1
2.2 TASK STATEMENTS	2-4
2.3 GROUND TRUTH	2-6
3. METHOD OF APPROACH	3-1
3.1 SITE GROUND TRUTH VERIFICATION	3-1
3.2 DATA RESAMPLING	3-2
3.3 DATA CATEGORIZATION	3-7
3.4 OUTPUT PRODUCT GENERATION	3-10
3.4.1 Color Categorized Images	3-10
3.4.2 Test Field Area Tables	3-18
4. INTERPRETATION OF RESULTS	4-1
4.1 CATEGORIZED IMAGERY	4-1
4.2 AREA TABULATIONS	4-2
4.3 SYSTEM POINT SPREAD FUNCTIONS (PSF) AND MODULATION TRANSFER FUNCTIONS (MTF)	4-5

CONTENTS (CONT.)

	<u>Page</u>
5. CONCLUSIONS AND RECOMMENDATIONS	5-1
5.1 CONCLUSIONS	
5.2 RECOMMENDATIONS	
APPENDIX A POINT SPREAD FUNCTIONS AND MODULATION TRANSFER FUNCTION	A-1
APPENDIX B REFERENCES	B-1

## ILLUSTRATIONS

<u>Figure</u>	<u>Title</u>	<u>Page</u>
2-1	Ground Truth Map of Test Area	2-7
2-2	Color Infrared Mosaic of Test Area	2-8
3-1	LANDSAT PSF Overlayed on the Sample Point	3-4
3-2	Two Dimensional Procedure	3-6
3-3	Categorized Imagery - Original LANDSAT Data	3-11
3-4	Categorized Imagery - Cubic Convolution Original Sampling Interval	3-12
3-5	Categorized Imagery - Bendix Restoration Original Sampling Interval, Assumed S/N = 30	3-13
3-6	Categorized Imagery - Bendix Restoration Original Sampling Interval, Assumed S/N = 2	3-14
3-7	Categorized Imagery - Cubic Convolution 40 x 40 Meter Sampling Interval	3-15
3-8	Categorized Imagery - Bendix Restoration 40 x 40 Meter Sampling Interval, Assumed S/N = 30	3-16
3-9	Categorized Imagery - Bendix Restoration 40 x 40 Meter Sampling Interval, Assumed S/N = 2	3-17

## TABLES

<u>Table</u>	<u>Title</u>	<u>Page</u>
2-1	Tabulation of Categorized Data and Ground Truth for LANDSAT Data	2-9/2-12
3-1	Area of Test Fields (Hectares) Resampling Interval of 56.9 x 79.1 Meters	3-22
3-2	Area of Miscategorized Boundaries (Hectares) Resampling Interval of 56.9 x 79.1 Meters	3-23
3-3	Area of Test Fields (Hectares) Resampling Interval of 40 x 40 Meters	3-24
3-4	Area of Miscategorized Boundaries (Hectares) Resampling Interval of 40 x 40 Meters	3-25
4-1	Normalized Field Area Estimates	4-4
4-2	Boundary Miscategorization Normalized for Two Resampling Intervals	4-5

SECTION 1  
INTRODUCTION AND SUMMARY

1.1 BACKGROUND

The evolution of the satellite earth observation program for natural resources from experimental to operational usage has placed increasingly stringent demands upon the cartographic accuracy of the output products of the ground processing facilities. The transition of users from imagery products to digital products has made it necessary to consider digital correction techniques to be applied to the computer-compatible tape products generated by the ground processing facilities. NASA and the Department of the Interior, in acceding to the data user requirements, have been considering techniques to be used in the digital geometric correction of satellite earth observation data for dissemination to data users. Present plans of NASA and the Department of the Interior <sup>(1)</sup> call for digital resampling of the data from the LANDSAT series of satellites into a format defined as the Space Oblique Mercator <sup>(2)</sup> coordinate system using the "cubic convolution" resampling technique as the method for geometric correction of the data.\* This technique was selected from the then known candidates as the most suitable candidate for geometric resampling of the LANDSAT satellite data with minimum degradation of the spectral and radiometric quality of the original satellite data.

To retrace our steps a bit, Bendix initiated an investigation in late 1973, as part of its on-going company-sponsored research, to develop a technique to merge LANDSAT scenes of the same geographical area for change detection and temporal processing applications. The two alternatives were to develop techniques to autocorrelate two LANDSAT scenes for merging, or to

---

\*References are located in Appendix B.

merge two scenes by geometrically correcting each scene to a common geographical coordinate system. Bendix selected the latter course as the preferred alternative, and began evaluation of resampling techniques to accomplish the objective. The then commonly known resampling techniques included "nearest neighbor", spline fit, bilinear interpolation,  $\text{Sin } X/X$ , and cubic convolution. Each of these techniques was basically an interpolation technique which attempted to derive a radiometric value for a new picture element location by interpolating the values of the original array of data to determine a value for a new element not existing in the original array. These interpolation techniques tended to degrade either the radiometric quality or the spatial resolution of the data during the resampling process. Radiometric degradation would tend to reduce the performance of categorization algorithms for earth resources applications problems, while spatial degradation would increase the minimum resolvable feature size and/or cause fringing around features when two resampled scenes were merged.

Bendix had previously developed<sup>(3)</sup> a technique for increasing the spectral resolution of digital spectrometer data which involved developing a computer model of the data collecting instrument and deconvolving the spectrometer data to reduce or remove the effects of the convolution of the original scene caused by the spectral resolution limitations and electronic characteristics of the spectrometer. Bendix decided to develop a new resampling technique for LANDSAT data which incorporated this deconvolution concept (rather than interpolation) and which would minimize spatial and radiometric degradation of the data during resampling for geometric correction. This technique<sup>(4)</sup>, which Bendix calls "restoration" to differentiate the technique from interpolation techniques,



has yielded performance characteristics which exceed the original Bendix expectations. The technique does indeed appear to provide a geometric resampling approach for LANDSAT data which does not have the performance drawbacks of the known interpolation techniques. In addition, at the user's option, the technique appears capable of improving either the spatial or radiometric characteristics of the original data set, or a combination of both.

In early 1976, Bendix informed NASA of the existence of the technique and its apparent performance characteristics. NASA expressed interest in Bendix restoration as a prospective geometric resampling technique for future earth resources satellite data, and in March 1976 awarded Bendix a contract to perform a comparative evaluation of the Bendix restoration technique and cubic convolution. This report describes the conduct of that project and the results.

## 1.2 PROJECT OBJECTIVE

The objective of the contract was to perform a quantitative comparison of cubic convolution and Bendix restoration as LANDSAT data resampling techniques for geometric correction of the data. Since the intended usage of the candidate technique is for generation of geometrically corrected digital data tapes for dissemination to earth resources data users, it was elected to perform the quantitative comparison based upon evaluation of accuracy of categorized (classified) data. The categorization was to be performed with identical training fields using identical ground truth information after the original LANDSAT data sets were resampled using the two techniques. It was believed by both Bendix and NASA that evaluation of categorized data would be the most stringent comparison of the performance of the two techniques, and that the evaluation methodology could be established to yield quantitative comparison information requiring little in the way of investigator interpretation.

### 1.3 SUMMARY OF RESULTS

The data selected for use in the project was LANDSAT II data collected over a LACIE (Large Area Crop Inventory Experiment) test site in Finney County, Kansas on July 6, 1975. These data were selected because detailed ground truth information was available on the site, and the site had been flown with color IR photography within a few days of the LANDSAT overpass.

The data were resampled using both cubic convolution and Bendix restoration with the original data sampling interval and a 40-meter sampling interval. The original data and the resampled data were all categorized using common ground truth and common training sites. The categorization accuracy was reviewed and only test fields which correlated well between categorization, ground truth, and aerial photography were selected for further evaluation.

The evaluation methodology used was to compare identical fields in the different sets of data and tabulate the apparent areas of the fields and the apparent areas of boundary miscategorization between the fields. The tabulations were produced by generating area tables of portions of the data sets containing the test fields. Five fields or areas were selected where the pixels associated with the fields under investigation and the boundaries between the fields and their surrounds could be unambiguously identified in area table computer printouts. This technique was used because the tradeoffs between the different resampling techniques would be most clearly demonstrated by evaluating performance on small fields and their boundaries, where spatial/radiometric data quality is most critical, and computer printouts could be obtained, on a pixel-by-pixel basis, of identical areas in the different sets of data.

Comparison of the field areas and the extent of field boundary miscategorization clearly indicated that the Bendix restoration resampled data, when compared to the cubic convolution resampled data, provided a better estimate of the area of the test fields and less miscategorization at the boundaries between fields. Additionally, the Bendix restoration technique permits tradeoffs between spatial resolution and radiometric quality in the resampling process. Several combinations of spatial and radiometric resolution were arbitrarily selected for use during the evaluation. Some of the combinations indicated under evaluation that performance superior to that achieved with the original, unresampled LANDSAT data was being achieved.

The conclusions reached were that:

1. The Bendix restoration technique was superior to cubic convolution as a LANDSAT resampling technique. Improvements varied from 7 to 56% under different conditions.
2. There were indications that Bendix restoration improved categorization performance compared to the original data set.
3. There were likely to be optimum tradeoffs between spatial/radiometric quality during resampling for different earth resources applications and/or an optimum tradeoff for most applications. However, the study was not of sufficient depth to ascertain optimization parameters.

A parallel study performed by Bendix showed that, if implemented in a special-purpose hardware processor, restoration throughput rates would be similar or identical to a cubic convolution hardware processor with a slight increase in hardware complexity. When implemented in machine language software for this project, restoration run times were 10 to 20% longer than cubic convolution run times.

Section 2 of this report describes the scope of effort of the project. Section 3 describes the method of approach. Section 4 presents the interpretation of the results of the processing. Section 5 presents the conclusions derived from the project and recommendations for further activity. Supporting data are provided in Appendix A.

## SECTION 2

### PROJECT OBJECTIVE AND SCOPE OF EFFORT

#### 2.1 PROJECT OBJECTIVE

The objective of the contract was to perform a quantitative comparison of cubic convolution and Bendix restoration as LANDSAT data resampling techniques. Although the resampling techniques are intended for use in digital geometric operations, evaluation of geometric considerations was not the issue. Any resampling technique, since it synthesizes new pixels to generate a geometrically correct array of digital data, will modify the pixel data in the process. The issue under investigation was the effect of the resampling process upon the accuracy of computer categorization (classification) using standard computer categorization techniques.

A number of resampling techniques exist. Most are interpolation techniques designed to provide the best estimate of a data value located between original data values through methods which are basically linear or nonlinear curve fitting techniques. Because cubic convolution has been selected by NASA as the resampling technique to be used in future digital resampling of LANDSAT data, cubic convolution was used to represent interpolative approaches to resampling.

Bendix has developed a resampling technique which is not interpolative in nature. That is, it does not assume that the best intermediate pixel value should be derived by curve fitting the existing data set. The Bendix restoration technique attempts to determine what the scanner video value should have been at the desired sample point through knowledge of the optical

and electronic transfer characteristics of the scanner, their likely effects upon data values surrounding the desired resampled data point, and assumptions concerning the scanner signal-to-noise ratio and degree of correlation between terrain features within the scanner field of view. Consequently, the Bendix approach is a deconvolution technique rather than an interpolation technique. Therefore, the project objective could be stated to be a comparison between interpolation as a resampling technique versus deconvolution as a resampling technique. Since deconvolution is attempting to estimate the best radiometric signal values for a new sample as seen by the scanner rather than the best interpolation between two values on a data tape, the technique comparison must involve performance evaluation against actual terrain features or a reasonable analog, rather than comparisons between the "original" data tapes and resampled data tapes. Further, the possibility that the resampled data tape could be different but better than the "original" data tape must be considered, since the basis of comparison is actual terrain features.

The most realistic approach to comparison of the two techniques appeared to be through the use of spectral pattern recognition techniques. That is, a set of data resampled with each of the techniques would be subjected to computer categorization (classification) for land or vegetation cover categories, compared to detailed ground truth of the test area, and evaluated based upon conformance to the ground truth. For the comparison to be quantitative, several conditions must be met:

- A. Identical resampling intervals must be used over identical test areas to assure identical numbers of pixels in comparable test areas.
- B. Identical training sets must be used for the development of the coefficients used for categorization.
- C. Categorization must be performed on the same system under identical conditions.
- D. Because both spatial and radiometric comparisons are to be made, small features and sharp, definable transitions from one feature to another must exist in the data.
- E. As detailed ground truth as possible concerning the size, shape, and contents of features on the surface of the earth must be available for comparison and evaluation.
- F. A method of comparison must be used to compare feature categorization to ground truth information for exactly the same area on the surface of the earth, based upon pixel count and/or feature area.

To meet the above conditions, the test site selected for the performance of the project was a portion of a LACIE (Large Area Crop Inventory Experiment) test site in Finney County, Kansas. LANDSAT II data of the test site was collected

on July 6, 1975. Ground truth consisting of false color infrared photography, detailed tabulations of the agricultural content of fields, tabulations of areas of the fields, and maps of the test site were available.

Using this LANDSAT data and ground truth, the project objectives were to be met by resampling the LANDSAT data using cubic convolution and Bendix restoration, categorizing the original and resampled data using identical training sets, and comparing the areas of test fields (by counting pixels) to the actual areas of the same fields determined from maps and/or physical area measurements. Further, to evaluate both spatial and radiometric performance of the resampling techniques, particular emphasis was to be placed on the evaluation of categorization performance at the boundaries between fields containing different crops or surface cover.

## 2.2 TASK STATEMENTS

The tasks to be performed in the conduct of the projects are described below. It should be noted that the described tasks are modified slightly from those in the original contract. The modifications were jointly agreed upon by NASA and Bendix and were performed to permit evaluation of Bendix restoration using more than one combination of spatial versus radiometric restoration. To provide funds for the additional resampling processing performed in Task 1, some reduction in scope was made in the interpretation task (Task 4).

Task 1. Perform resampling processing of LANDSAT data over the supersite test area (approximately 5 miles E-W or 120 pixels by 7 miles N-S or 160 pixels) with the following parameters:

Using cubic convolution:

Original LANDSAT sampling interval (approximately 57 x 79 meters)

40 x 40 meter sampling interval.



Using Bendix restoration:

Original LANDSAT sampling interval, assumed S/N ratio = 2

Original LANDSAT sampling interval, assumed S/N ratio = 30

40 x 40 meter sampling interval, assumed S/N ratio = 2

40 x 40 meter sampling interval, assumed S/N ratio = 30

Task 2. Perform categorization analysis of LANDSAT data using selected training sets from within the LACIE supersite area for each agricultural category. Other categories (not agricultural) may use common training data from without the supersite region, selected from the unprocessed LANDSAT CCT's. This analysis will be performed on each of the resampled data sets generated in Task 1, plus the original LANDSAT data. Output will be categorized CCT's and color-coded categorized images.

Task 3. Provide area error measurements for individual fields for each case. GS will provide ground truth data to be used for this task. These data will define field boundaries, areas, and crops for the test area. For each case, the contractor will provide tabulations of individual field area measurements for the category assigned to the crop of this field. This measured area will be differenced from the ground truth area to obtain an area measurement error. The number of fields measured and tabulated may be less than the total fields in the test area, based on cost limitations of this contract.

Deliverable output products of this task will be the error tabulations for each case and graphical presentations of this data.

Task 4. Provide interpretation of accuracy data tabulations. Tasks 1 through 3 primarily provide NASA with objective data relative to the performance improvements achievable by the Bendix LANDSAT data restoration method (Objective 1). This task provides a separable interpretation of these results by the personnel most directly involved in performing the study.

### 2.3 GROUND TRUTH

For a project of this type, accurate ground truth is extremely important, since small variations between categorizations of the same geographical locations are being sought. Consequently, Bendix took extreme care in verification of the accuracy and utility of the ground truth.

NASA supplied a map of the test area, reproduced in Figure 2-1, a series of color infrared aerial photographs of the test area, copied in Figure 2-2, and a series of tabulations of individual fields obtained by ground survey (not illustrated). Bendix carefully cross-examined the three sources of ground truth data and rejected use of any fields which did not correlate in all three sources. Bendix also examined color composite images of the LANDSAT data, interpreted the images, and rejected any test fields which did not appear to conform to the ground truth. Finally, Bendix categorized the original LANDSAT data and rejected any fields from analysis and interpretation which did not appear to conform to the ground truth. The information used to perform this step is shown in Table 2-1. Bendix believes the resultant winnowed ground truth information used in this project is of unquestionable accuracy and ground truth errors have a negligible effect upon the results and conclusions of the project.

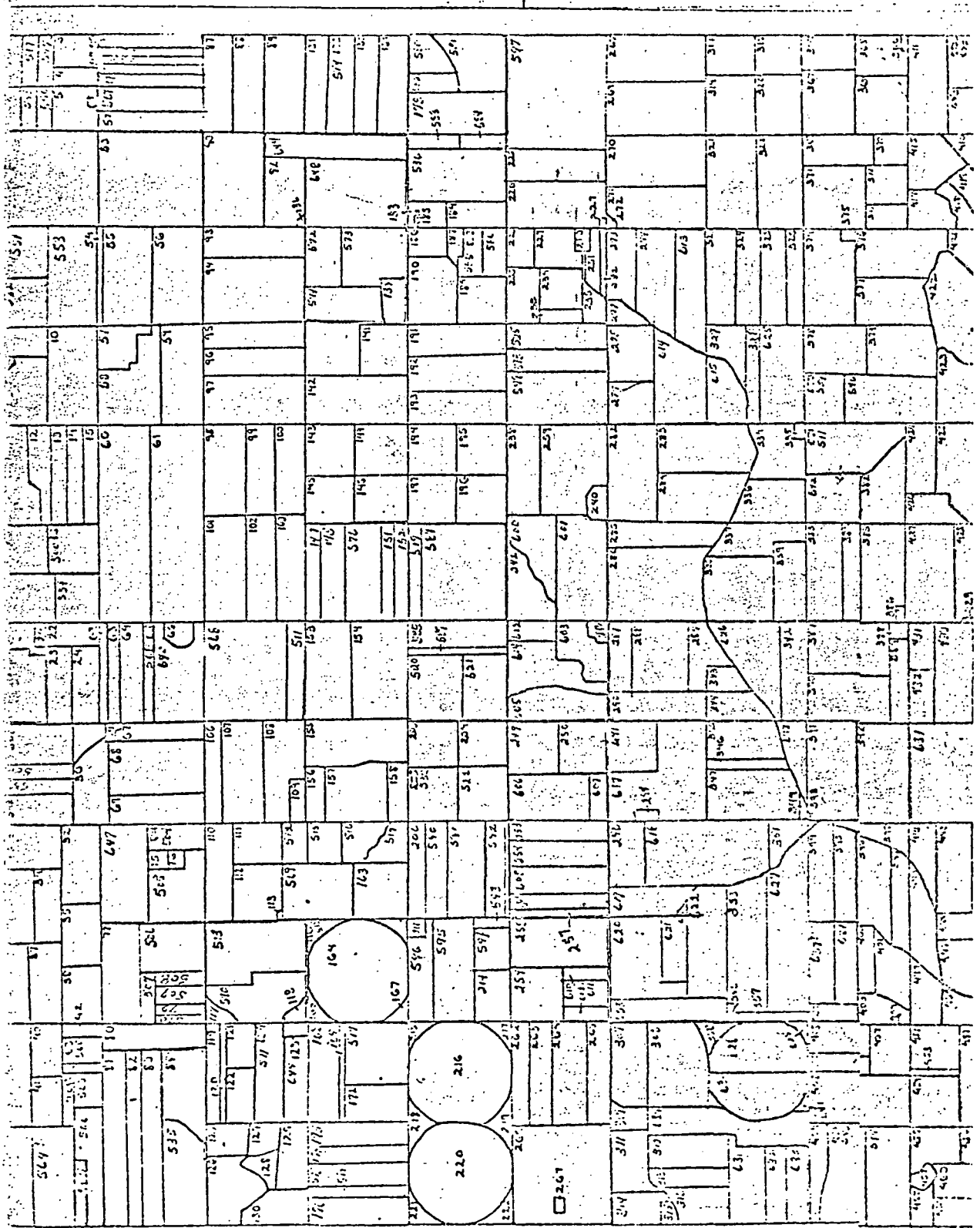


Figure 2-1 Ground Truth Map of Test Area

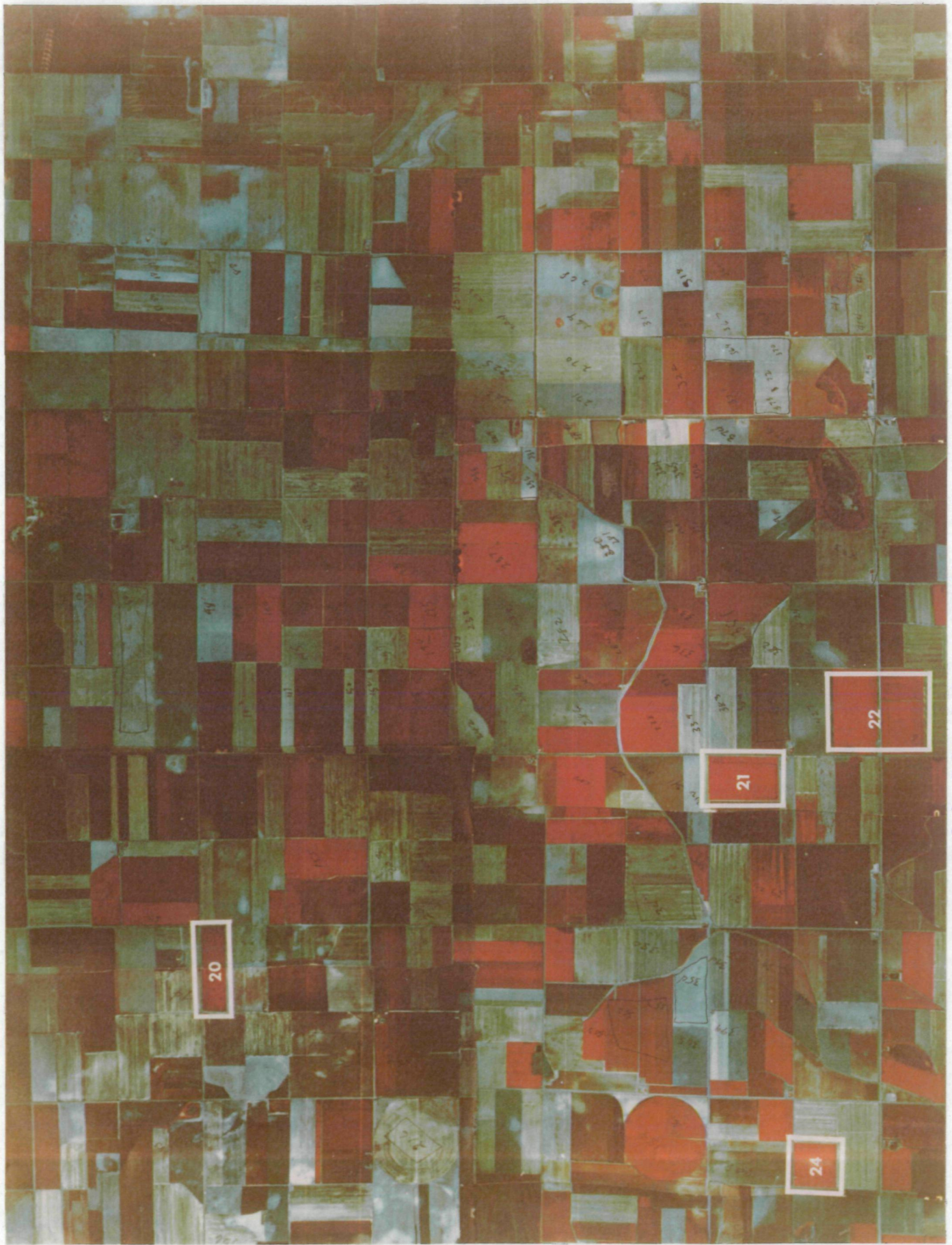


Figure 2-2 Color Infrared Mosaic of Test Area

TABLE 2-1

Evaluation of Categorized Data and Ground  
Truth for LANDSAT Data

<u>Field No.</u>	<u>Color</u>	<u>Correct</u>		<u>Field Structure</u>	<u>Notes</u>
		<u>Yes</u>	<u>No</u>		
318 W.W.	Brown	X		Good	
320 Corn	Yellow	X		Good	
364 Corn	Yellow	X		Good	
367 W.W.	Brown	X		Fair	
369 W.W.	Brown	X		Good	
371 C	Yellow	X		Good	
321 Alf	Blue		X		Cloud Shadow
374 S.F.	Blue	X		Good	
378 G.S.	Magenta	X		Fair	
380 Corn	Yellow	X		Good	Field Representation differs between ground truth and photography
336 Alf	Pink	X		Good	
351 Corn	Yellow	X		Good	
338 Alf	Pink	X		Good	
339 W.W.	Brown	X		Good	
383 W.W.	Brown	X		Good	
387 Alf	Pink	X		Good	
390 G.S.	Magenta	X		Good	
391 W.W.	Brown	X		Good	
394 W.W.	Brown/ Yellow	?		Poor	Small field possibly harvested
395 G.S.	Yellow		X	Poor	Field structure does not correlate with ground truth

TABLE 2-1 (CONT.)

<u>Field No.</u>	<u>Color</u>	<u>Correct</u>		<u>Field Structure</u>	<u>Notes</u>
		<u>Yes</u>	<u>No</u>		
537/339 W.W.	Brown	X	X	Good	Field structure does not correlate with ground truth
405 G.S.	Yellow		X	Good	
408 S.T.	Magenta			Good	
410 C	Yellow	X		Good	
220 S.T.	Blue			Good	
174 W.W.	Brown	X		Good	
173 W.W.	Brown	X		Good	
171 Corn	Yellow	X		Good	
214 W.W.	Blue	X	X	Good	Ground truth wrong
212 Corn	Yellow	X		Good	
164 W.W.	Brown	X		Good	
206 8-	Yellow				
207 Corn	Yellow	X		Good	
203 W.W.	Brown	X		Good	
155 Alf	Pink	X		Good	
154 W.W.	Brown	X		Good	
200 S.F.	Blue	X		Good	
197 W.W.	Brown	X		Good	
194 Corn	Yellow	X		Good	
146 Corn	Yellow	X		Good	
144 Corn	Yellow	X		Good	
142 Corn	Yellow	X		Good	

TABLE 2-1 (CONT.)

<u>Field No.</u>	<u>Color</u>	<u>Correct</u>		<u>Field Structure</u>	<u>Notes</u>
		<u>Yes</u>	<u>No</u>		
141 Corn	Yellow	X		Good	
193 Alf	Pink	X		Good	
192 W.W.	Brown	X		Good	
191 Corn	Yellow/ Pink	X	X	Good	
190 W.W.	Brown	X		Good	
134 G.S.	Yellow		X	Good	
178 W.W.	Brown	X		Good	Field structure does not correlate with ground truth
177 S.F.	Blue/ Magenta/ Brown	X	X	Good	Field structure does not correlate with ground truth
88 W.W.	Brown	X		Good	
87 W.W.	Brown	X		Good	
90 W.W.	Brown	X		Good	
53 W.W.	Brown	X		Good	
56 W.W.	Brown	X		Good	
93 W.W.	Brown	X		Good	
94 W.W.	Brown	X		Good	
95 W.W.	Brown	X		Good	
59 W.W.	Brown	X		Good	
61 S.F.	Blue	X		Good	
68 Corn	Yellow	X		Fair	

TABLE 2-1 (CONT.)

<u>Field No.</u>	<u>Color</u>	<u>Correct</u>		<u>Field Structure</u>	<u>Notes</u>
		<u>Yes</u>	<u>No</u>		
69 Alf	Pink	X		Good	
110 Alf	Pink	X		Fair	
74 W.W.	Brown	X		Good	
80 S.F.	Blue	X		Good	
84 CLT	Blue	X		Good	
83 W.W.	Brown	X		Good	
126 W.W.	Brown	X		Good	
60 W.W.	Brown	X		Good	



SECTION 3  
METHOD OF APPROACH

3.1 SITE GROUND TRUTH VERIFICATION

The data selected for use in this project were LANDSAT II data collected over the LACIE test site in Finney County, Kansas on July 6, 1975. These data were selected because detailed tabular ground truth, in terms of field size and contents, was available on the site and false color infrared photography flown within a few days of the satellite overpass was available. The data for the test area were split between tapes 3 and 4 of the LANDSAT II Scene 2165-16453. Data sufficient to cover an area bigger than and including the test site were created by merging data from tapes 3 and 4. Initial categorization was carried out using the Bendix Multispectral Data Analysis System (MDAS). Thirteen distinct categories were selected and training sets for these categories that correlated well with aerial photography and ground truth were used in the categorization procedure. Interactive steps in selecting the training sets, categorization, and testing of the homogeneity of the training sets were carried out until a satisfactory level of categorization was achieved. This initial categorization was performed to verify the ground truth and to select training set fields to be used with all data sets in subsequent operations. The evaluation of this initial categorization was presented in Section 2 of this report. When resampling was performed as a later step, the starting point for resampling was chosen to be the 8th element and the 8th scan line of the original merged LANDSAT data. For the case of all the original sampling intervals, 500 elements and 397 scan lines were created in each case. For the case of all 40-meter sampling intervals, 700 elements and 780 scan lines were created in each case. Thus there was one-to-one correspondence in coordinates among the cases of the original sampling interval data and the 40-meter sampling interval data. This ensured that the training

sets selected to carry out the categorization came from the same fields by means of a check of the coordinates of the training fields. Every effort was made to select the same areas in each field so that the effects of training set variations from one case to another case was minimized.

### 3.2 DATA RESAMPLING

LANDSAT digital data contains geometric distortions due to a number of sources (scanner or spacecraft parameters, etc.) and is not in a geographically (earth) oriented coordinate system. To be useful for mapping purposes, the data must be geometrically corrected. The geometric correction, whether to remove scanner distortion or to correct the data to a specified map projection, is accomplished by resampling the digital data. The digital data have already been sampled on the spacecraft in the process of digitizing to provide a series of pixels ordered along scan lines and as a series of scan lines (rows and columns). The resampling process converts the digital data into a new series of pixels and scan lines where the locations of the pixels conform to a specified location on the surface of the earth rather than a location in scanner coordinates. Obviously, the sample points corresponding to locations on the surface of the earth will not correspond to sample points in scanner coordinates. Further, the original sampling was done at specified times in the scan line and the scanning was also done in the time domain (so many scans per second) yielding a nominal but varying sampling interval on the earth's surface (56.9 x 79.1 meters). The resampling can be done using a different sampling interval on the ground (40 x 40 meters, etc.), or the same sampling interval as the nominal interval. The resampling process by itself does not directly affect the ground resolution of the data, but the resampling technique does. The purpose of this project was to compare the

effects on the data quality of the Bendix "restoration" resampling technique and the cubic "convolution" resampling technique.

Cubic convolution is an interpolation technique which is a 4 point by 4 point approximation to the  $\sin x/x$  infinite set of coefficients which are theoretically correct for interpolating regular point samples of a band-limited input function.

The aim of the Bendix restoration process is to estimate as accurately as possible what the true radiometric value of the ground was at the point in question, not simply to make an interpolative estimate of what the LANDSAT output would have been if it had happened to have looked directly at that point. Two necessary inputs to the process are the scanner point-spread function (PSF) and the detailed pixel pattern in the region of the point. From the dimensions of the ends of the fiber-optic bundle in the scanner, the focal length, the mirror velocity, the optical blur function, and the response of the three-pole Butterworth filter in the sensor electronics, the effective point-spread "smear" on the ground has been computed. Although no direct measurements of the PSF have been possible, scenes which have been processed using the synthesized PSF model show improvements which confirm the validity of the model.

By digitally centering the PSF on the point to be restored, the amount of information contained in each of the underlying pixels relative to the resample point can be determined. Figure 3-1 shows a typical LANDSAT PSF overlaid on an array of image data. Notice that the contribution by each pixel around the resample point is the projection onto the PSF curve. The restoration process then takes this information along with other inputs related to the signal/noise ratio of the data, the degree of correlation between adjacent pixels, the desired output PSF, and the number of pixels which will be used in the restoration array, and computes a set of coefficients which, when applied to the radiometric values of the surround-

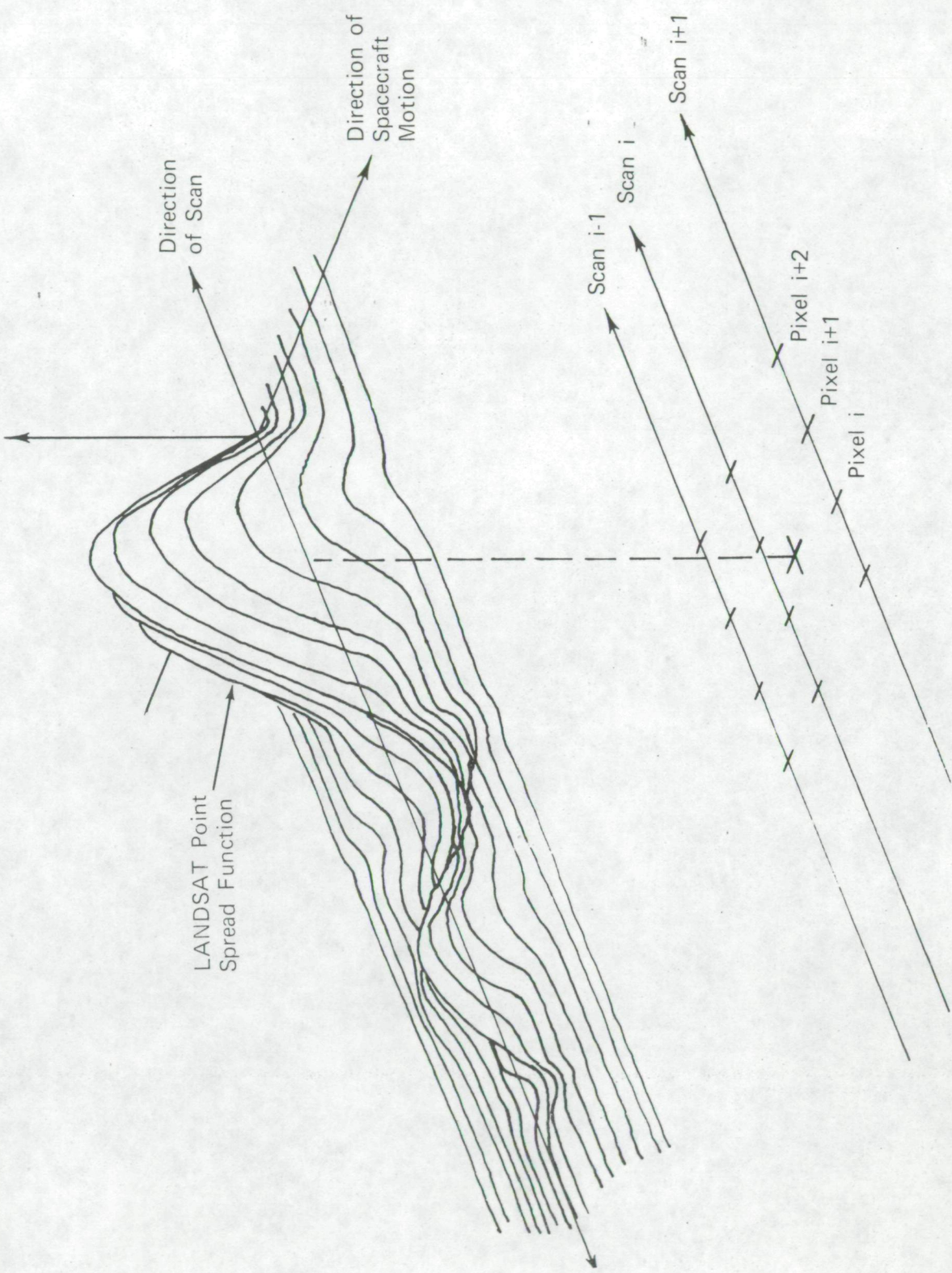


Figure 3-1 LANDSAT PSF Overlaid on the Sample Point

ing pixels and summed, give the best estimate of the original ground radiometric value at the resample point.

The Bendix restoration algorithm creates 10 sets of 8 and 4 coefficients for use in the along-scan direction and across-scan direction, respectively. These coefficients were derived based on the LANDSAT scanner PSF, presented in Appendix A, and on the desired sampling interval and assumed signal-to-noise ratio. The assumed signal-to-noise ratio is not the raw scanner signal-to-noise ratio, but the noise with respect to the digital data range for the features to be discriminated. These coefficients were determined by a method of least squares in order to minimize radiometric and geometric errors. Synthetic PSF's, which are the product of the scanner PSF's and restoration coefficients, give a visual picture of the weights of neighboring pixels in determining the radiometric values of the pixels in question.

For cubic convolution, 10 sets of 4 coefficients for use in both along and across scan directions were derived. Cubic convolution utilizes 16 data values to compute one data point. This procedure, thus, neither takes into account the scanner PSF nor does it provide for noise considerations in the image.

The original data were restored using Bendix restoration at both the original sampling interval and 40-meter sampling interval. Signal-to-noise ratios of 2.0 and 30.0 were arbitrarily selected and used for each sampling interval. The data were also resampled using cubic convolution at the original and 40-meter sampling interval. The resampling algorithm for both the Bendix restoration and cubic convolution applied corrections for earth's rotation, but not for detector-to-detector misregistration of fractional pixels that are present in the original data.

Referring to Figure 3-2, the appropriate set of 8 along-scan coefficients were applied to each of the scan lines, yielding preliminary estimates for the circled positions. Four cross-scan coefficients are then applied to these, completing the process for the given pixel for the location indicated by the x as an example. Synthetic PSF's, which are the product of the scanner PSF and restoration coefficients, give a visual picture of the weights of the neighboring pixels, both in magnitude and sign, in determining the radiometric value of the pixel in question. Plots of the scanner PSF and their MTF's in the across-track  $n$  and along-track directions are presented in Figures 1 and 2 (Appendix A), respectively.

Plots of two sets each of across-track and along-track PSF's and MTF's, one positioned on the original pixel and one positioned midway between pixels, for each combination of the sampling interval and signal-to-noise ratio are presented in Figures 3 through 18, Appendix A.

In the case of cubic convolution, coefficients were created by fitting a cubic polynomial to a  $\sin X/X$  function.<sup>(5)</sup> Along track and across-track coefficients were the same for each of the 10 sub-pixel intervals. An array of  $4 \times 4$  pixels was used to determine the radiance of the given pixel with a procedure similar to the one described for Bendix Restoration.

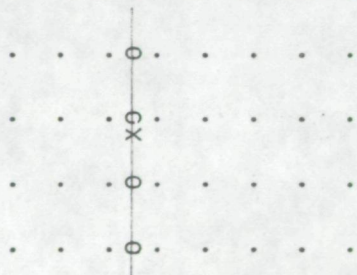


Figure 3-2 Two-Dimensional Procedure

At the completion of the resampling portion of the project, the following six resampled data sets of the identical ground area were available:

<u>Resampling Technique</u>	<u>Resampling Interval</u>
Cubic Convolution	40 x 40 meters
Cubic Convolution	56.9 x 79.1 meters
Bendix Restoration, SN = 2, SN = 30	40 x 40 meters
Bendix Restoration SN = 2 , SN = 30	56.9 x 79.1 meters

### 3.3 DATA CATEGORIZATION

The original data from LANDSAT II was categorized using the Bendix Multi-spectral Data Analysis System (MDAS). The same fields that were used in categorizing the original data were also used in categorizing resampled data.

The processing steps used in categorizing are briefly summarized below.

#### Establish Significant Categories

The first step in the categorization procedure was to locate and designate to the computer a number of picture elements that typified each category. The areas of known categories were established from ground truth and infrared aerial photography. The training areas were located on the CCT's by viewing the CCT data on the MDAS TV monitor under false color combination of bands 4, 5 and 7, and under single band color sliced display of band 7 data. Training sets for each category were selected by carefully examining the ground truth with LANDSAT imagery. Only those training fields whose

LANDSAT imagery correlated well with all three sources of ground truth, namely the map, aerial photography, and field tabulations of individual fields from ground survey, were selected. The coordinates of the training areas were then designated to the computer by placing a cursor over the desired area, assigning a training area designation, category code, color code, and name. One training set each for each of the 13 categories were selected. The color code was used in later playback of the tapes when the computer categorized data are displayed in the designated colors.

#### Develop Processing Coefficients

The LANDSAT spectral measurements within the training area boundaries were edited by the computer from the CCT and processed to obtain a numerical descriptor (computer-processing coefficients) to represent the spectral characteristics of each land cover category. The descriptors included the mean signal and standard deviation for each of the four bands and the covariance matrix taken about the mean. The descriptors were then used to generate a set of processing coefficients for each category. In multivariate categorical processing, the coefficients are used by the computer to form a linear combination of the measurements for each pixel. The variable produced has an amplitude which is associated with the probability that the unknown pixel measurements belong to each of the particular land cover categories sought. In categorical processing, the probability of a pixel arising from each one of the different land cover categories of interest is computed for each pixel and a decision, based on these computations, is reached. If all the probabilities are below a threshold level specified by the operator, the computer will decide that the



category viewed is unknown, or "uncategorized".

#### Evaluate Selection of Training Areas and Processing Coefficients

Before producing categorized data a number of tests were applied to evaluate the computer's ability to perform the desired interpretation. The tests included generating categorization-accuracy tables and viewing the processed imagery on the MDAS TV monitor. Selection of training areas, generation of accuracy tables, and evaluation of processing results through use of computer printouts and the TV monitor were iterative operations.

#### Categorize Resampled Data

Categorization for the resampled cases were carried out using common ground truth and training sets from the same fields as in the case of the original data. A field-by-field evaluation, however, was not carried out for the resampled data.

### 3.4 OUTPUT PRODUCT GENERATION

The results of the resampling processing, training set selection, and categorization were a set of categorized CCT's for the six resampling cases. Each categorized CCT contained the same number of pixels as the appropriate resampled data tape, but the four bands of MSS data were replaced with a single pixel coded as one of the thirteen categories used or as an uncategorized pixel (none of the thirteen).

Two types of output products were generated from the categorized CCT's: color categorized images, and area tables.

#### 3.4.1 Color Categorized Images

A color image was generated for each of the data sets. These images, shown in Figures 3-3 through 3-9, used the same colors for the categories as were used on the MDAS display. Three categories of corn, 6 categories of wheat, 2 categories of summer fallow, sorghum and alfalfa were used for categorization. The color code for these categories is the same for all data sets and is provided below:

Wheat	- Brown
Wheat (late maturity)	- Medium gray
Corn	- Yellow
Alfalfa	- Pink
Sorghum	- Magenta
Summer Fallow	- Bright blue

The images were generated as color separation negatives on an Optronics P-1500 drum film recorder. The color separation negatives were then registered



Fig. 3-3 Categorized Imagery - Original LANDSAT Data

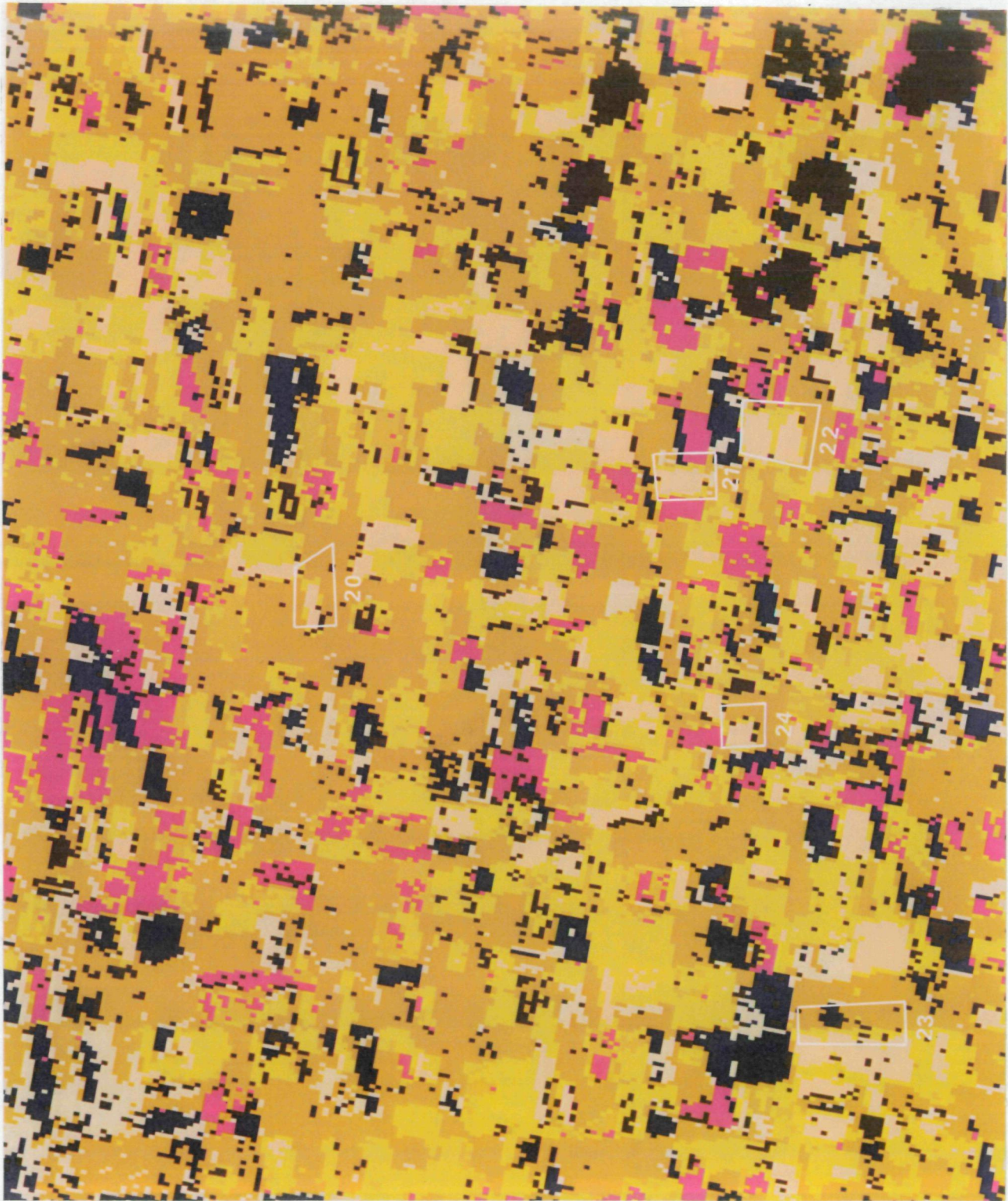


Fig. 3-4 Categorized Imagery - Cubic Convolution  
Original Sampling Interval



Fig. 3-5 Categorized Imagery - Bendix Restoration  
Original Sampling Interval, Assumed  $S/N = 30$



Fig. 3-6 Categorized Imagery - Bendix Restoration  
Original Sampling Interval, Assumed  $S/N = 2$

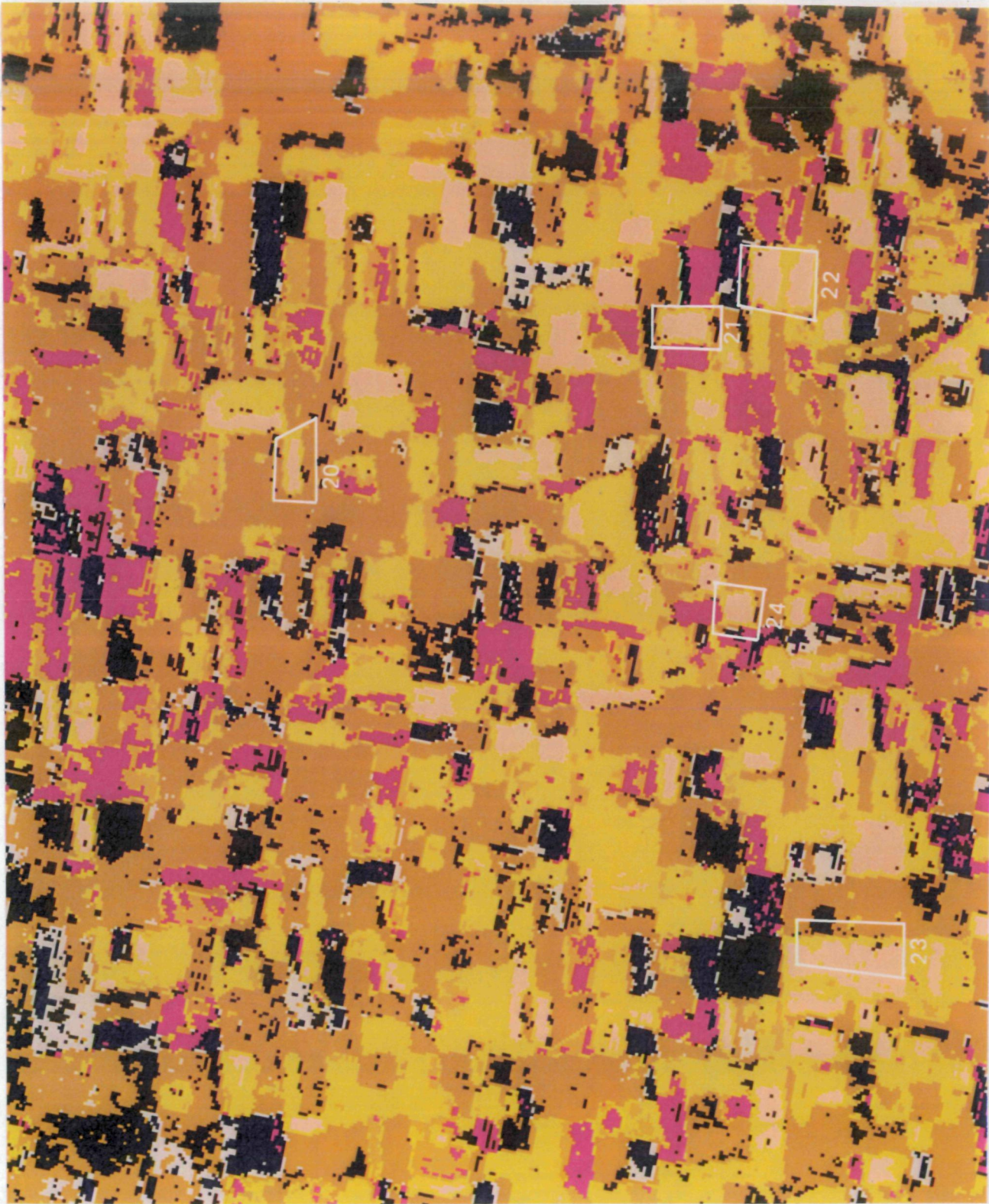


Fig. 3-7 Categorized Imagery - Cubic Convolution  
40 x 40 Meter Sampling Interval



Fig. 3-8 Categorized Imagery - Bendix Restoration  
40 x 40 Meter Sampling Interval, Assumed S/N = 30





Fig. 3-9 Categorized Imagery - Bendix Restoration  
40 x 40 Meter Sampling Interval, Assumed S/N = 2

onto color film and the appropriate separation negatives were exposed onto the color film with red, green, and blue light to generate a color positive transparency. An internegative was then made from the positive transparency and enlarged color prints made from the internegatives. Insofar as possible, the color prints were made to the same scale. Because the images include the original LANDSAT data interval plus two different resampling intervals, and the drum recorder is digital with fixed recording apertures, the scaling was done with a combination of recording aperture selection and photographic enlargement.

Annotated on the images are five test fields or areas identified as areas 20 through 24. The use to which these areas were put are described in the next subsection.

#### 3.4.2 Test Field Area Tables

A feature of the Bendix MDAS is the ability to generate "area tables". The cursor used for training set selection can also be used to delineate an area on the CRT display and the system computer will generate a table for the area enclosed by the cursor, listing the percent coverage of each category contained within the cursor. Also listed are the coverage of the area by category in acres and square kilometers. The area for each category is determined by counting the number of pixels for each category and multiplying the number of pixels by the area per pixel. This feature of MDAS was used to generate quantitative data tables for later use in evaluating the different sets of resampled data.

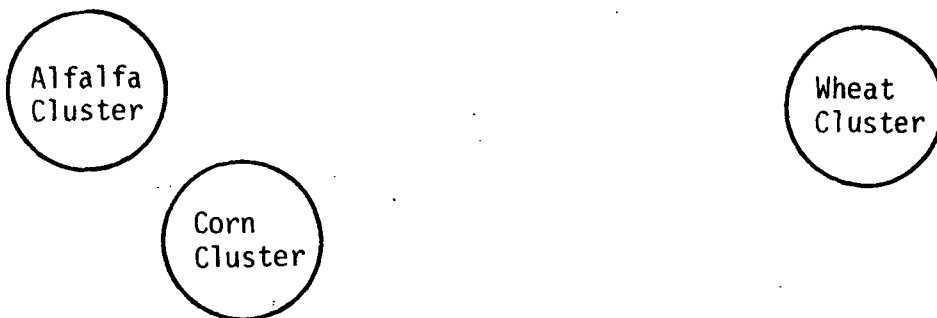
One of the sources of error in the use of categorized LANDSAT data for resources inventory is miscategorization due to mixtures of terrain features at the boundaries of fields. As the MSS video signal is being sampled and digitized in the spacecraft, inevitably transitions from one terrain feature type to another will be encountered. A typical encounter is the boundary between two agricultural fields containing different crop types. As the sampling and digitizing process proceeds along a scan line, one sample may appear to occur near the boundary of a field but not touch it, the next sample may appear to be directly astride the boundary (obviously containing information from both crop types), while the next sample or pixel may appear to be completely in the new field and not contain information from the previous field. No one will argue that the pixel astride the boundary between two fields, obviously containing information from two crop types, could be categorized as either one or the other crop type, or as another crop type entirely whose signature (spectral characteristics) is similar to a mixture of the two crop types. However, even a casual examination of Figure 3-3, which shows categorized LANDSAT data at the original sampling interval, will find many field boundaries which contain miscategorization two or more pixels wide. Why does this occur? Reference to Figure 3-1, which illustrates the LANDSAT point spread fraction with reference to a sampling grid, or any of the PSF curves shown in Appendix A shows that any pixel contains information from areas beyond those of the immediate apparent location of the pixel in question. Because a pixel in an image does not appear to be in a position to be affected by a boundary does not mean that it is not affected. The pixel size shown in an image is related to the sampling interval, not to the size of the ground area affecting that particular data sample. The

data sample could contain ground information from terrain as many as three sampling intervals away. Further, use of a resampling technique to digitally correct the data from a geometric standpoint can make the matter worse. An extreme example would be the case where the sampling interval is indeed equal to the ground footprint of the scanner, the samples occur on either side of a boundary with neither sample containing information from the field across the boundary, and the data are resampled using linear interpolation for a new pixel halfway between the two original pixels.

This discussion addresses the major issue of this project. Does Bendix restoration as a resampling technique provide results superior to cubic convolution? To address this problem, five test areas were selected which all exhibited the same characteristics. The fields selected for evaluation were alfalfa fields completely surrounded by wheat (with the exception of one area, not a field, which was a border between a wheat field and an alfalfa field). These fields were selected for the following reasons:

- A. There was no corn in the area being evaluated, only wheat and alfalfa.
- B. The spectral signature of corn is similar to alfalfa (but separable).

The "clusters" associated with alfalfa and wheat are widely separate. The "cluster" associated with corn is in between the "clusters" for wheat and alfalfa in signature space and is close to the "cluster" for alfalfa, as shown below.



If a pixel is on a boundary between a wheat and an alfalfa field and contains a mixture, it will likely be categorized as corn. Further, since the corn cluster is closer to alfalfa than wheat, a small amount of wheat mixed with alfalfa will categorize as corn but a small amount of alfalfa mixed with wheat will still categorize as wheat. When resampling the boundaries of alfalfa and wheat fields, using either cubic convolution or Bendix restoration, a small amount of mixing is inevitable because the resampled pixel is obtained by multiplying an array of original LANDSAT pixels by processing coefficients to achieve the proper values for the resampled pixel. Bendix selected the alfalfa fields, surrounded by wheat, for test purposes because all corn pixels that appear are improperly categorized, or in error, since no corn exists in the areas selected.

The MDAS cursor was positioned for each of the areas marked on the images so that it was beyond the boundaries of the fields, and area tables were generated of the area inside the cursor. Both the apparent areas of the alfalfa fields and the apparent areas of the miscategorized boundaries (assuming the entire area listed as corn was boundary) were calculated and the results are presented in Tables 3-1 through 3-4. These tables have been converted from acres to hectares. The "field number" listings are from the ground truth tabulations originally provided. The "table number" identification is shown on the categorized images and the false color IR photomosaic included in this report.

Table 3-1  
 Area of Test Fields (Hectares)  
 Resampling Interval of 56.9 x 79.1 Meters

Field Nr.	Table Nr.	S/N = 30	S/N = 2	CC	Orig.	Actual Size
110	20	10.78	8.98	9.88	10.78	18.18
387	21	22.00	19.30	19.76	20.21	26.31
428	22	42.21	41.31	44.00	43.55	57.8*
--	23	22.00	21.10	13.92	22.45	--
454	24	13.47 88.46	11.67 81.26	11.67 85.31	13.92 88.46	19.42 121.71

\*Measured from Map

○ Deleted from Totals

Table 3-2  
 Area of Miscategorized Boundaries (Hectares)  
 Resampling Interval of 56.9 x 79.1 Meters

Field Nr.	Table Nr.	S/N = 30	S/N = 2	CC	Orig
110	20	7.18	5.39	6.29	6.29
387	21	6.29	14.37	10.33	9.88
428	22	13.92	19.76	15.72	16.61
--	23	10.24	8.98	13.02	9.88
454	24	3.14	10.78	6.29	5.39
		40.77	59.28	51.65	48.05

Table 3-3  
 Area of Test Fields (Hectares)  
 Resampling Interval of 40 x 40 Meters

FIELD NR.	TABLE NR.	S/N = 30	S/N = 2	CC	ORIG	ACTUAL SIZE
110	20	11.2	9.12	9.92	10.78	18.18
387	21	21.44	19.2	18.72	20.21	26.31
428	22	42.4	41.44	40.8	43.55	57.8*
--	23	23.52	25.28	20.48	22.48	--
454	24	13.92	11.2	12.64	13.92	19.42
		88.96	80.96	82.08	88.46	121.71

\* Measured from Map

○ Deleted from Totals



Table 3-4  
 Area of Miscategorized Boundaries (Hectares)  
 Resampling Interval of 40 x 40 Meters

FIELD NR.	TABLE NR.	S/N = 30	S/N = 2	CC	ORIG.
110	20	7.52	8.0	11.36	6.28
387	21	8.8	12.32	14.08	9.87
428	22	16.0	16.86	19.2	16.59
	23	12.16	11.2	15.36	9.87
454	24	5.6	6.72	10.08	5.38
		50.08	55.1	70.08	47.99

## SECTION 4

### INTERPRETATION OF RESULTS

#### 4.1 CATEGORIZED IMAGERY

Photo analysis of the categorized imagery with ground truth reveals that the fields are better defined in terms of shape, and boundaries between fields are more accurately classified in the Bendix restored data than in the cubic convolution. Furthermore, the categorization procedure is more discriminating, especially for the Bendix restored data with assumed S/N of 30 with 40-meter sampling interval, than either the cubic convolution or the case of S/N of 2. Given the alternative between miscategorizing vs. not categorizing, the Bendix restored data with S/N of 30 ends up with more instances of uncategorization than miscategorization. The amount of uncategorized pixels in the restored data with assumed S/N of 30 also indicates that more categories need to be chosen when the radiometric quality is improved so that the uncategorized pixels can be properly assigned their proper categories. In other words, if the data have improved radiometric quality, then more categories are required to completely categorize the data. For example, the left part of the field below test field 20 is shown more as uncategorized in the Bendix restored data (S/N = 30) than other data sets. Aerial photography confirms that field is different from test field 20, and no training sets were selected to categorize this type of field. This qualitative assessment, that Bendix restored data with a resampling interval of 40 meters with assumed S/N ratio of 30 is superior to both cubic convolution and the original data, is backed up by the quantitative assessment that follows.

## 4.2 AREA TABULATIONS

The fields selected for area tabulations are identified as "table numbers" 20 through 24 in Tables 3-1 through 3-4 of Section 3 of this report. These same fields are identified in the categorized imagery shown in Figures 3-3 through 3-9.

The fields selected were small in area to emphasize boundary effects. Consequently, for several fields, the area of miscategorized boundary cells is of similar magnitude to the area categorized as the fields. Further, the miscategorized boundary cells (categorized as corn) are generally alfalfa cells in actuality. This effect makes the categorized areas of the fields much smaller than the area as measured from the maps. The large mensuration errors should not be a cause for alarm. The investigation was not conducted to evaluate the ability of LANDSAT to identify agricultural crops, but to compare resampling techniques. Consequently, fields were selected by size and crop type to exaggerate differences between resampling techniques.

Two types of tables were generated for evaluation. One type was tabulations of the categorized areas of each of the test fields for comparison to the actual sizes of the fields. The second type of tabulation was the areas of the miscategorized boundaries. This last statement is not strictly true since all "corn" pixels are assumed to be in the miscategorized boundary and occasional "corn" pixels occurred within the fields.

Referring to Tables 3-1 and 3-3, the criterion for judging the resampling alternatives is the largeness of the categorized fields. That is, the larger the categorized area of the field for each case, the better the performance. On the average, the Bendix restoration ( $S/N = 30$ ) area is larger

than areas for cubic convolution for both 56.9 x 79.1 meter and 40 x 40 meter resampling intervals, and Bendix restoration ( $S/N = 2$ ) is smaller for both resampling intervals. This observation is not true on a field-by-field basis but field-to-field variations are assumed to be partially caused by where the resampling grid occurred with respect to the original sampling grid and the locations of the field boundaries with respect to the sampling and resampling grids. The same type of observations can be made about Tables 3-2 and 3-4, which compare areas of miscategorized boundaries by field for each resampling approach. In the case of these two tables, the smaller the area of miscategorization, the better the performance. For the two resampling intervals used, Bendix restoration ( $S/N = 30$ ) outperformed cubic convolution in both cases, and outperformed the original data for the 56.9 x 79.1 sampling interval. Bendix restoration ( $S/N = 2$ ) performed poorer than cubic convolution for the 56.9 x 79.1 resampling interval and better than cubic convolution for the 40 x 40 meter sampling interval.

These data can be presented in another way, as shown in Tables 4-1 and 4-2. These tables show only the original data, Bendix restoration ( $S/N = 30$ ), and cubic convolution. Additionally, the data have been normalized by dividing the areas by the measured areas of the fields, tending to reduce case-by-case variations due to the size range of the fields. Using this approach, the average of the normalized areas for the various fields was the same for Bendix restoration and the original data, and was 7 to 8% smaller for cubic convolution. This was true for both resampling intervals. For the miscategorized boundaries, the miscategorization was 19% smaller than the original data for

Bendix restoration at the 56.9 x 79.1 resampling interval. Cubic convolution yielded the same miscategorized area as the original data. For the 40 x 40 meter resampling interval, Bendix restoration gave the same miscategorized boundary area as the original data while the miscategorized area for cubic convolution was 56% larger.

The area tabulation data were also analyzed to see if any trends could be detected related to the aspects (height-to-width ratio) of the various fields, but no meaningful trends were evident.

Table 4-1  
Normalized Field Area Estimates

Field Number	Table Number	56.9 x 79.1 m			40 x 40 m		
		Orig. Data	Cubic Conv	Bx Rest.	Orig. Data	Cubic Conv	Bx Rest.
110	20	.59	.54	.59	.59	.54	.62
387	21	.76	.75	.84	.76	.71	.81
428	22	.75	.76	.73	.75	.71	.73
454	24	.72	.60	.69	.72	.65	.72
Avg Value		.71	.66	.71	.71	.65	.72
% Deviation From Original		-	-7%	0	-	-8%	+1

Table 4-2  
 Boundary Miscategorization  
 Normalized for Two Resampling Intervals  
 (56.9 x 79.1 and 40 x 40 meters)

Field Number	Table Number	56.9 x 79.1 m			40 x 40 m		
		Orig. Data	Cubic Conv	Bx. Rest.	Orig. Data	Cubic Conv	Bx. Rest.
110	20	.35	.35	.39	.35	.62	.41
387	21	.38	.39	.24	.37	.53	.33
428	22	.29	.27	.24	.29	.33	.27
454	24	.28	.32	.16	.27	.52	.29
Avg Value		.33	.33	.26	.32	.50	.32
% Deviation From Original		-	0	-19%	-	+56%	0

#### 4.3 SYSTEM POINT SPREAD FUNCTIONS (PSF) AND MODULATION TRANSFER FUNCTIONS (MTF)

The point spread function of the scanner is similar to, and looks much like, a slice through the blur circle plot of an optical system. The PSF, however, includes system effects such as the band limiting electronic filter, the sampling and digitizing functions, etc. The modulation transfer function is the spatial frequency response of the scanner. Both types of curves are included in Appendix A for the original LANDSAT data and for all the resampling approaches. For the resampled data, the PSF's and MTF's are included for both a new sample registered with (on top of) an old sample and a new sample taken landing between two original samples. Both along-track (direction of flight) and across-track (direction of scan) PSF's and MTF's are included. Reference to the descriptive illustration of the LANDSAT PSF (Figure 3-1) shows much less correlation between samples for along-track samples than for across-track samples. Consequently, Bendix restoration almost "nearest neighbor's" the along-track data (Ref. Figure 6, Appendix A) because of the low sample-to-sample correlation

in the along-track direction. In the across-track direction, the LANDSAT electronics and sampling intervals cause pixels removed some distance from the current sample to contain information relevant to that sample. Consequently, the restoration algorithm takes advantage of this correlation to construct a narrower PSF and a wider frequency response MTF.

Because of funding limitations, only two assumed signal-to-noise ratios were used in the study (2 and 30). From examination of the PSF's and MTF's, it appears that the two values "bracketed" the most desirable assumed S/N ratio. The S/N = 2 curves (Figure 11, Appendix A) compared to the LANDSAT PSF (Figure 2) appear to have the same PSF and a slightly degraded MTF. The S/N = 30 curves (Figure 4) show a narrower PSF and a wider frequency response, but there is a subsidiary peak in the MTF. The most desirable assumed S/N should be less than the 30:1 used but closer to 30:1 than 2:1, since 30:1 outperformed the lower value. There is not an easy way to evaluate the optimum S/N other than empirically. A modeling approach, if required, would involve an analysis of the spectral separability of all features to be categorized, using a methodology not clearly definable from the information available at present.

## SECTION 5

### CONCLUSIONS AND RECOMMENDATIONS

#### 5.1 CONCLUSIONS

The results of the project clearly demonstrated that LANDSAT data resampled using the Bendix restoration technique yielded higher classification accuracies and less miscategorization than LANDSAT data resampled using cubic convolution. This conclusion is supported by the results presented in Tables 3-1 through 3-4, Tables 4-1 and 4-2, and interpretation of the categorized imagery.

Interpretation of the categorized imagery also indicated that restoration improved the radiometric/spatial quality of the data. In the context of the method of approach for this project, this improvement detracted somewhat from interpretation of the results. The improvement provided more variability in the signatures of the various fields which led to larger numbers of uncategorized pixels. The variability was not an artifact because interpretation of the CIR photography confirmed that the increased variations observed existed in the fields.

Finally, it was concluded that an insufficient number of resampled cases were used to empirically explore the tradeoff parameters available with Bendix restoration to select an optimum combination. Two resampling intervals (56.9 x 79.1 meters and 40 x 40 meters) were used, and two assumed signal-to-noise ratios (2:1, 30:1) were used. Smaller resampling intervals and higher signal-to-noise ratios both appeared to improve performance.



For the resampling interval tradeoff, no clear indication of a desirable resampling interval was obtained; however, observation of along-track PSF's would lead to the conclusion that no significant advantage would be gained by making the resampling interval smaller than the original sampling interval in this direction. It is believed that improved performance would be obtained with smaller resampling intervals in the across-track direction.

Higher assumed signal-to-noise ratios improved performance. Of the two cases used ( $S/N = 2, 30$ ), the lower  $S/N$  ratio yielded poorer performance than the higher  $S/N$  ratios. However, examination of the PSF and MTF for  $S/N = 30$  seems to indicate the value chosen was too high and a value in the 20-25 range would be more appropriate to this problem. Other LANDSAT data and other terrain features may require different values.

## 5.2 RECOMMENDATIONS

From the results of this project, further experimentation certainly appears justified to determine both the optimum restoration tradeoff parameters for a particular set of data, and the likelihood of achieving an optimized set for all typical terrain features.

Secondly, a source of data for experimentation should be used whose characteristics are better defined than that used for this project. Use of actual data will tend to obscure the experimental results because of variations within fields and field-to-field variations. It is realized that such variations will be encountered in real life, but use of actual data in an experiment of this type detracted from the results because the variations are unquantified. It is known that GSFC has generated a synthetic data tape, with known variations,

for processing methodology evaluation. This data set would be a logical candidate for use in further experimentation.

Finally, the feasibility of modeling the problem should be investigated to reduce the need for iterative empirical evaluations for tradeoff analysis.

## APPENDIX A

### POINT SPREAD FUNCTIONS AND MODULATION TRANSFER FUNCTION

This appendix contains computer plots of LANDSAT MSS Point Spread Functions (PSF's) and Modulation Transfer Functions (MTF's) associated with the original MSS, and the synthesized functions representative of the Bendix restoration process and cubic convolution. The functions are shown for both along-track and across-track values when resampled positioned directly over a LANDSAT pixel and positioned midway between LANDSAT pixels.

A listing of the PSF's and MTF's included is as follows:

- Figure 1 Across-track Point Spread Function (PSF) of the LANDSAT Scanner and its MODULATION TRANSFER FUNCTION (MTF)
- Figure 2 Along-track PSF of the LANDSAT SCANNER and its MTF
- Figure 3 Across-track PSF and its MTF positioned on the pixel - S/N = 30, Original Sampling Interval
- Figure 4 Across-track PSF and its MTF positioned midway between pixels - S/N = 30, Original Sampling Interval
- Figure 5 Along-track PSF and its MTF positioned on the pixel - S/N = 30, Original Sampling Interval
- Figure 6 Across-track PSF and its MTF positioned midway between pixels - S/N = 30, Original Sampling Interval
- Figure 7 Across-track PSF and its MTF positioned on the pixels - S/N = 30, 40-Meter Sampling Interval
- Figure 8 Across-track PSF and its MTF positioned midway between pixels - S/N = 30, 40-Meter Sampling Interval
- Figure 9 Along-track PSF and its MTF positioned on the pixel - S/N = 30, 40-Meter Sampling Interval

- Figure 10 Along-track PSF and its MTF positioned midway between pixels -  $S/N = 30$ , 40-Meter Sampling Interval
- Figure 11 Across-track PSF and its MTF positioned on the pixel -  $S/N = 2$ , Original Sampling Interval
- Figure 12 Across-track PSF and its MTF positioned midway between pixels -  $S/N = 2$ , Original Sampling Interval
- Figure 13 Along-track PSF and its MTF, positioned on the pixel -  $S/N = 2$ , Original Sampling Interval
- Figure 14 Along-track PSF and its MTF positioned midway between pixels -  $S/N = 2$ , Original Sampling Interval
- Figure 15 Across-track PSF and its MTF, positioned on the pixel -  $S/N = 2$ , 40-Meter Sampling Interval
- Figure 16 Across-track PSF and its MTF positioned midway between pixels -  $S/N = 2$ , 40-Meter Sampling Interval
- Figure 17 Along-track PSF and its MTF, positioned on the pixel -  $S/N = 2$ , 40-Meter Sampling Interval
- Figure 18 Along-track PSF and its MTF positioned midway between pixels -  $S/N = 2$ , 40-Meter Sampling Interval
- Figure 19 PSF and MTF for Cubic Convolution  
- Positioned on the pixel, Original Sampling Interval
- Figure 20 PSF and MTF for Cubic Convolution  
- Positioned midway between pixels, Original Sampling Interval
- Figure 21 PSF and MTF for Cubic Convolution  
- Positioned on the pixel, 40-Meter Sampling Interval
- Figure 22 PSF and MTF for Cubic Convolution  
- Positioned midway between pixels, 40-Meter Sampling Interval

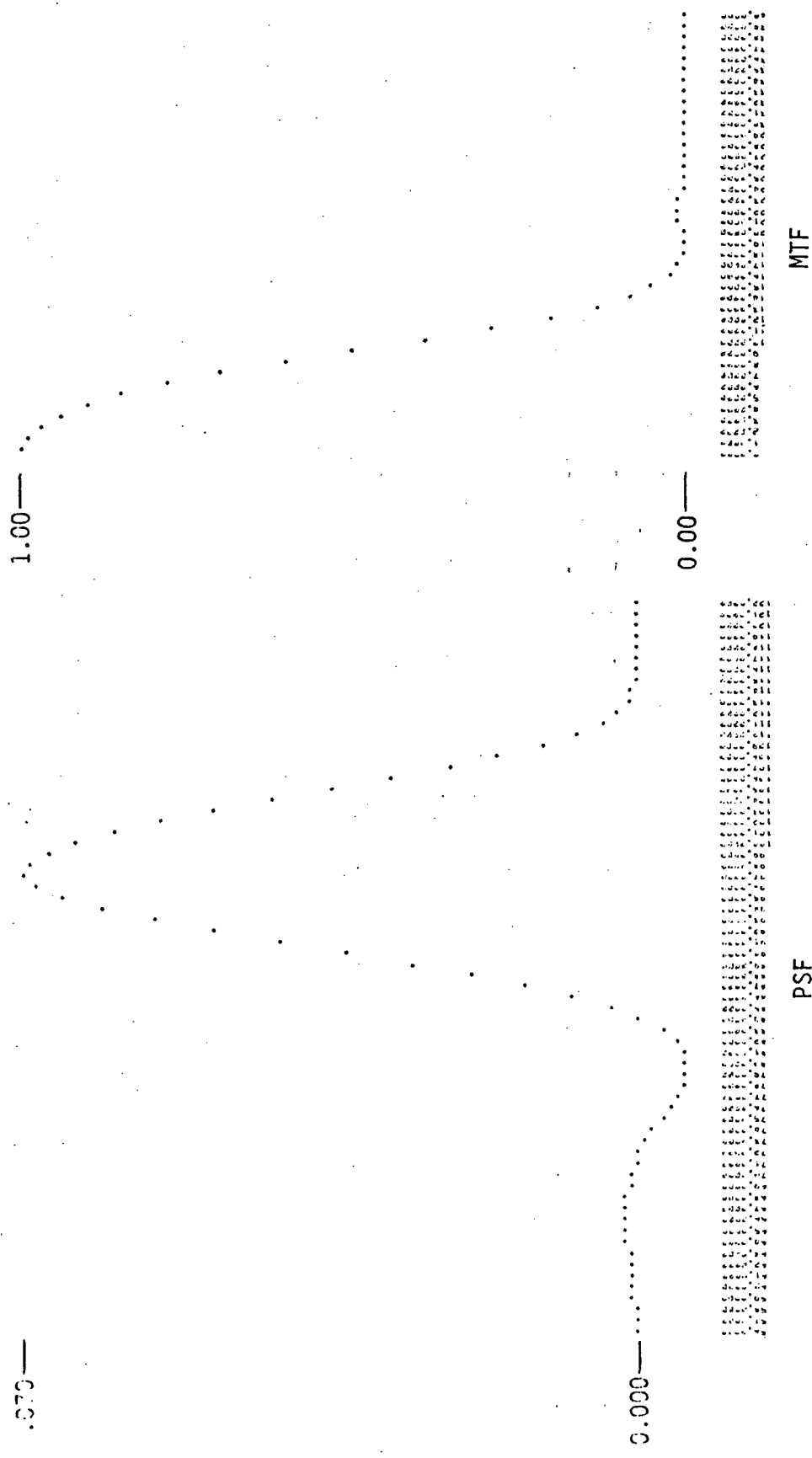


Figure 1 Across-Track Point Spread Function (PSF) of the LANDSAT Scanner and its MODULATION TRANSFER FUNCTION (MTF)

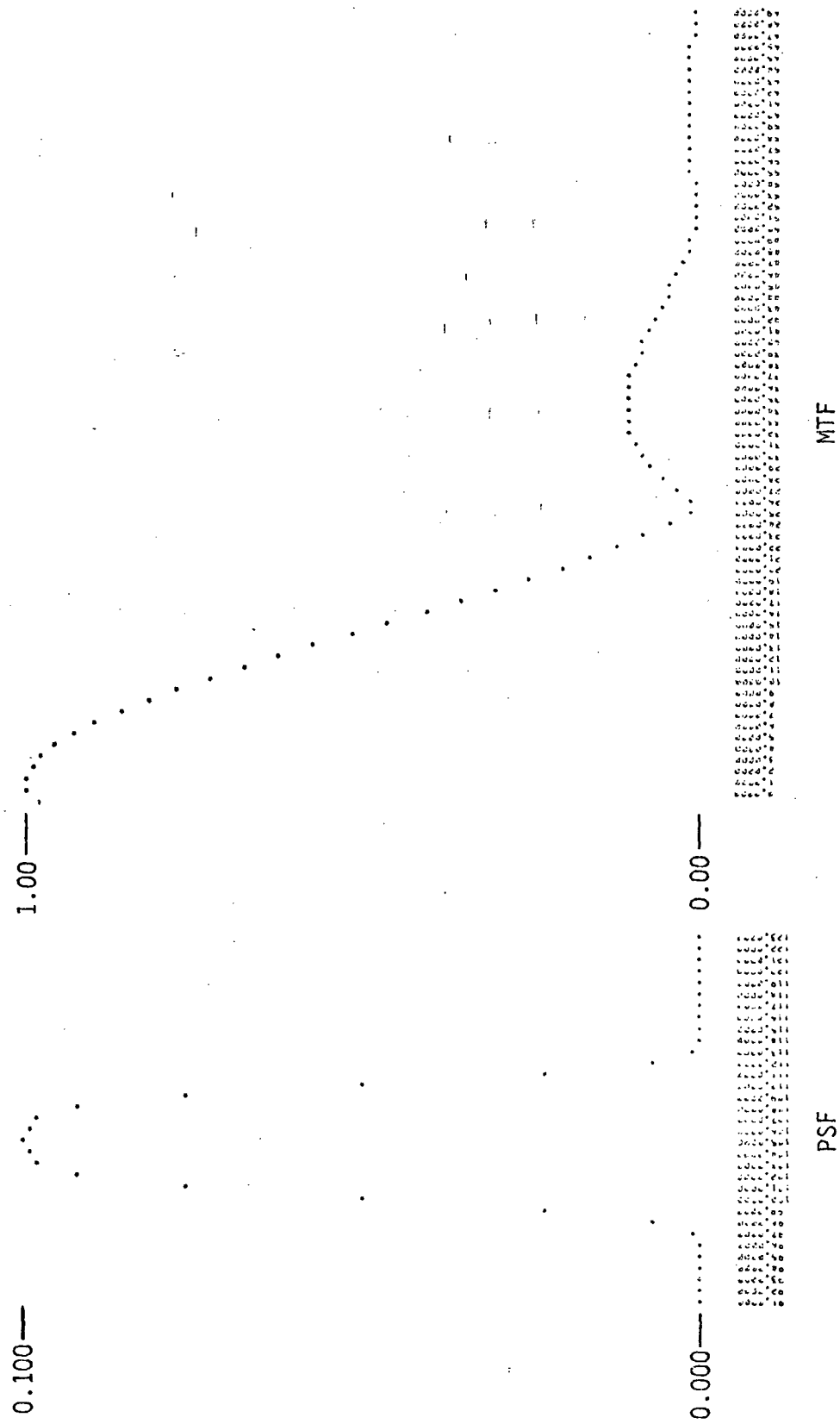


Figure 2. Along-Track PSF of the LANDSAT SCANNER and its MTF

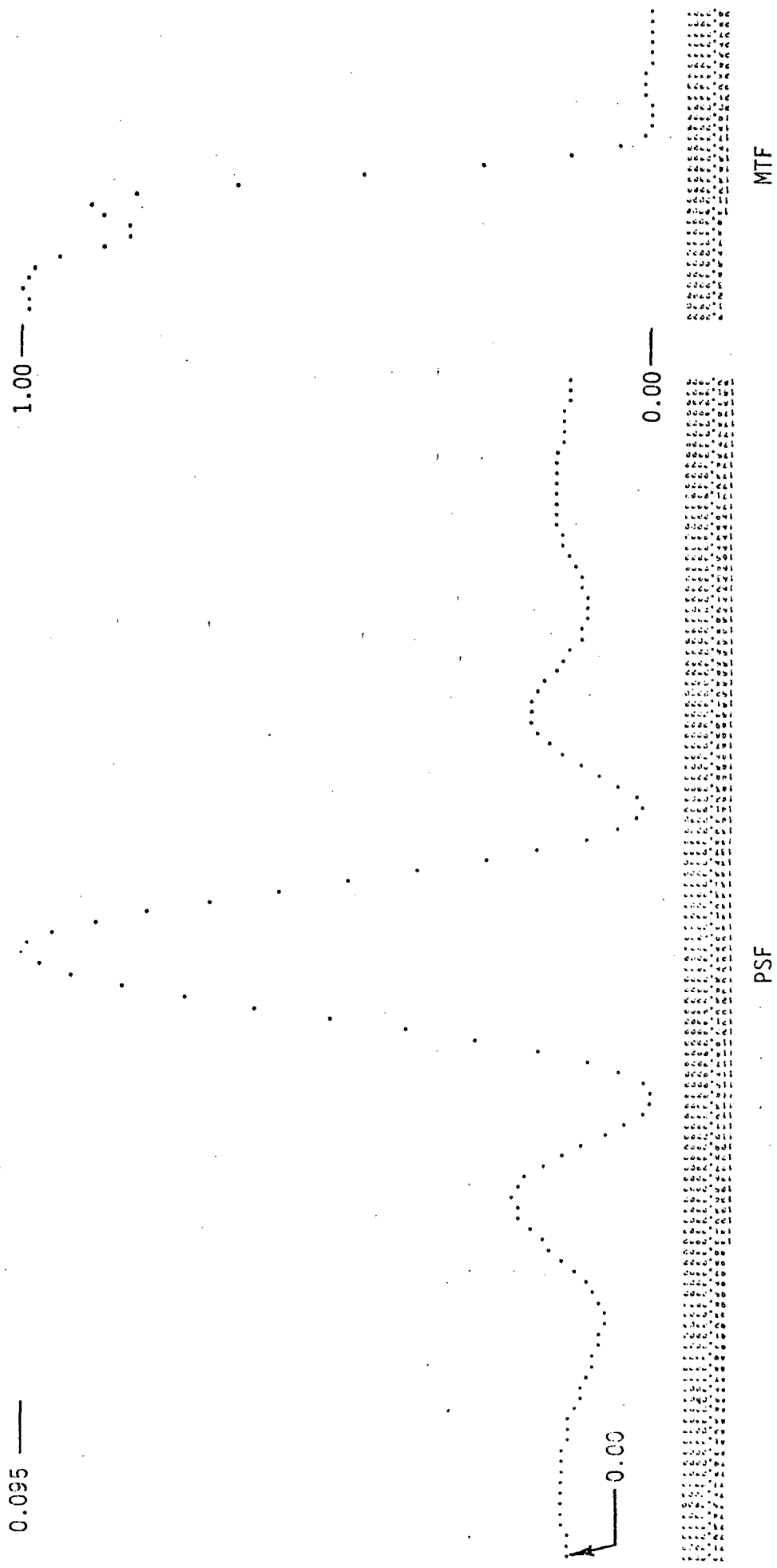


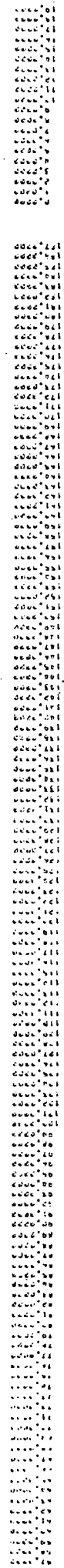
Figure 3 Across-Track PSF and its MTF Positioned on the Pixel  
 - S/N = 30, Original Sampling Interval

0.079 —

1.04 —

0.000 —

0.00 —



PSF

MTF

Figure 4 Across-Track PSF and its MTF Positioned Midway Between Pixels  
- S/N = 30, Original Sampling Interval



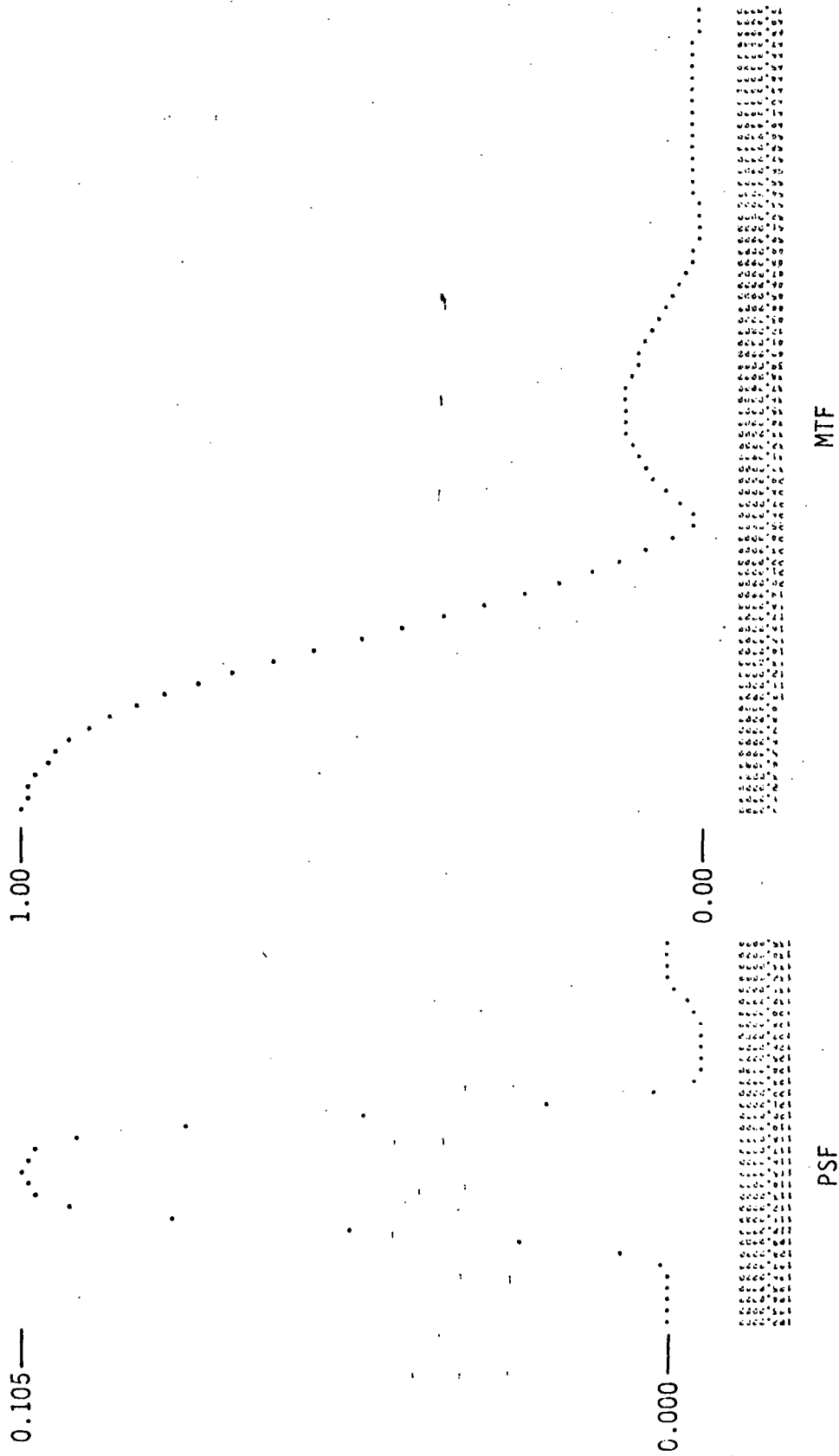


Figure 5 Along-Track PSF and its MTF Positioned on the Pixel  
 - S/N = 30, Original Sampling Interval

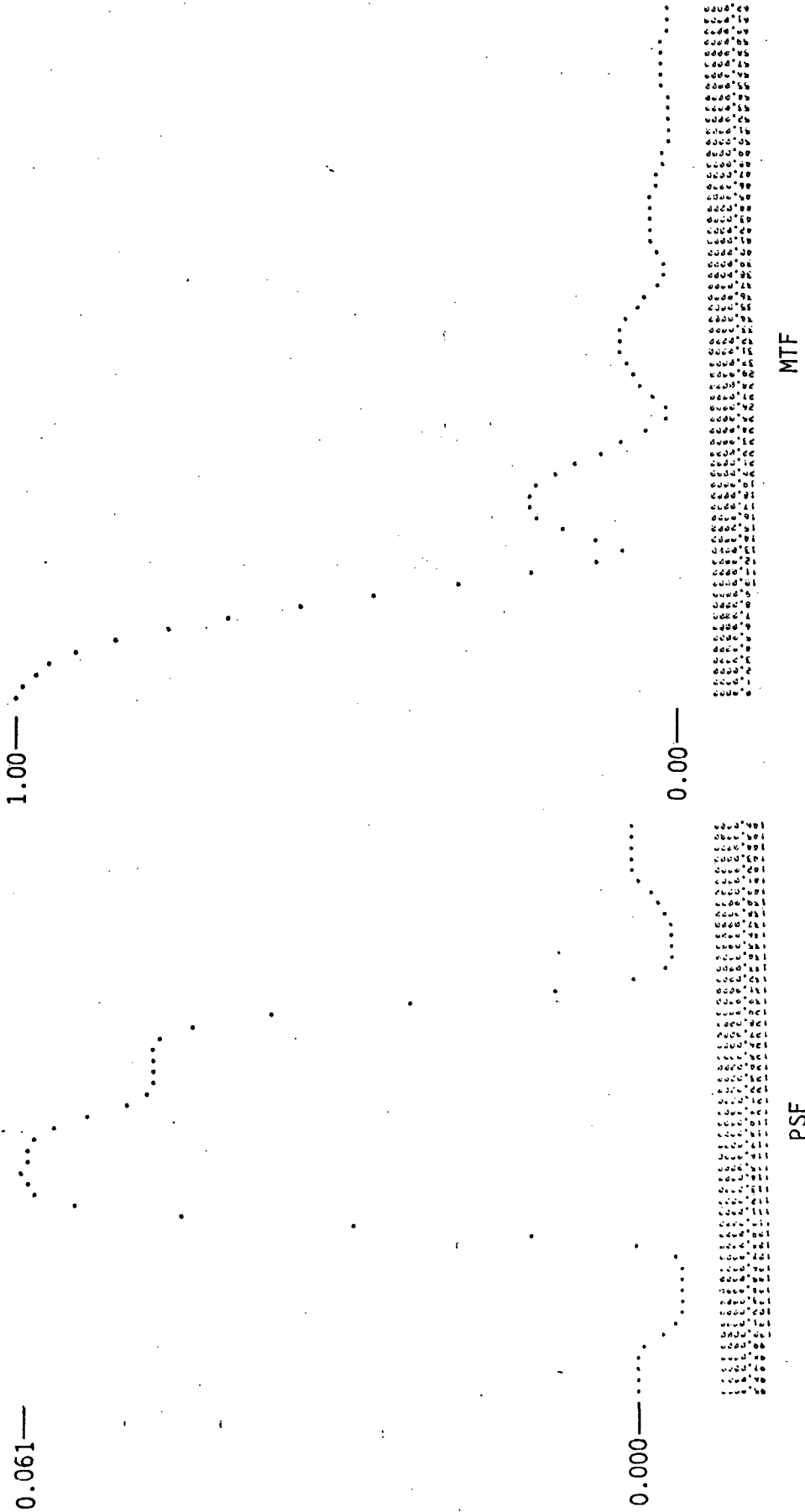
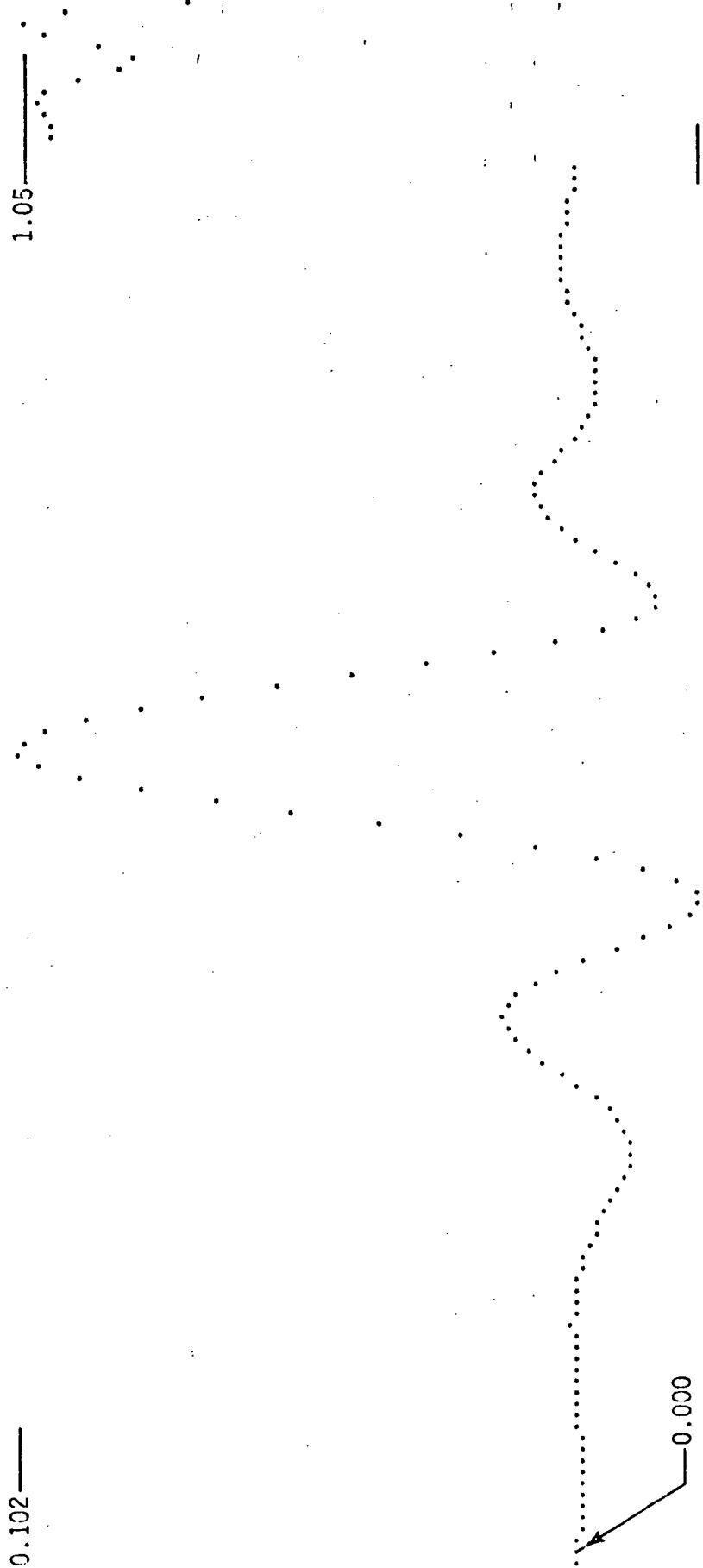


Figure 6 Along-Track PSF and its MTF Positioned Midway Between Pixels  
 - S/N = 30, Original Sampling Interval

0.102

1.05

0.000



0000'00  
0000'01  
0000'02  
0000'03  
0000'04  
0000'05  
0000'06  
0000'07  
0000'08  
0000'09  
0000'10  
0000'11  
0000'12  
0000'13  
0000'14  
0000'15  
0000'16  
0000'17  
0000'18  
0000'19  
0000'20  
0000'21  
0000'22  
0000'23  
0000'24  
0000'25  
0000'26  
0000'27  
0000'28  
0000'29  
0000'30  
0000'31  
0000'32  
0000'33  
0000'34  
0000'35  
0000'36  
0000'37  
0000'38  
0000'39  
0000'40  
0000'41  
0000'42  
0000'43  
0000'44  
0000'45  
0000'46  
0000'47  
0000'48  
0000'49  
0000'50  
0000'51  
0000'52  
0000'53  
0000'54  
0000'55  
0000'56  
0000'57  
0000'58  
0000'59  
0000'60  
0000'61  
0000'62  
0000'63  
0000'64  
0000'65  
0000'66  
0000'67  
0000'68  
0000'69  
0000'70  
0000'71  
0000'72  
0000'73  
0000'74  
0000'75  
0000'76  
0000'77  
0000'78  
0000'79  
0000'80  
0000'81  
0000'82  
0000'83  
0000'84  
0000'85  
0000'86  
0000'87  
0000'88  
0000'89  
0000'90  
0000'91  
0000'92  
0000'93  
0000'94  
0000'95  
0000'96  
0000'97  
0000'98  
0000'99

MTF

PSF

Figure 7 Across-Track PSF and its MTF Positioned on the Pixels  
- S/N = 30, 40-Meter Sampling Interval

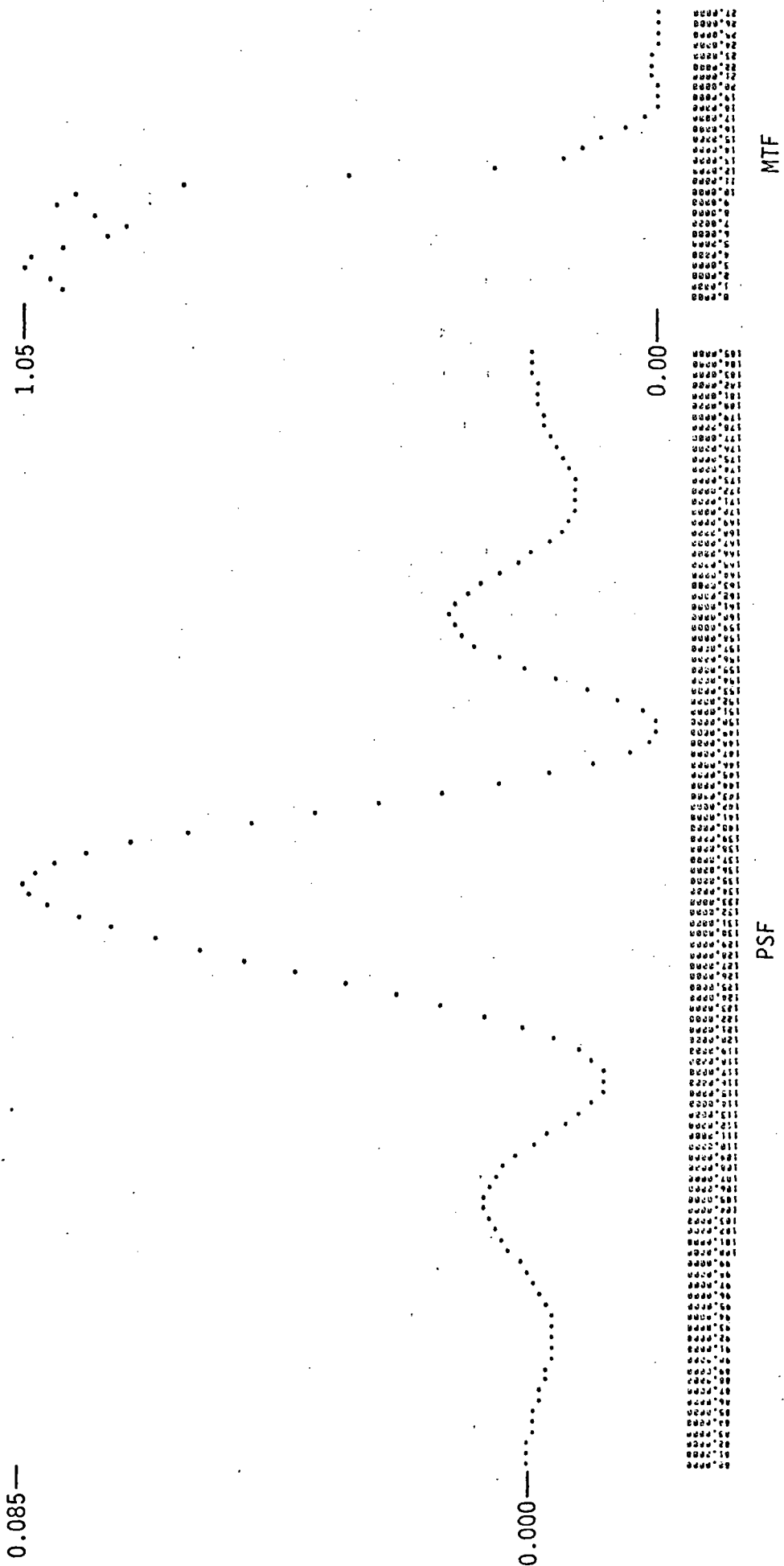


Figure 8 Across-Track PSF and its MTF Positioned Midway Between Pixels  
 - S/N = 30, 40-Meter Sampling Interval

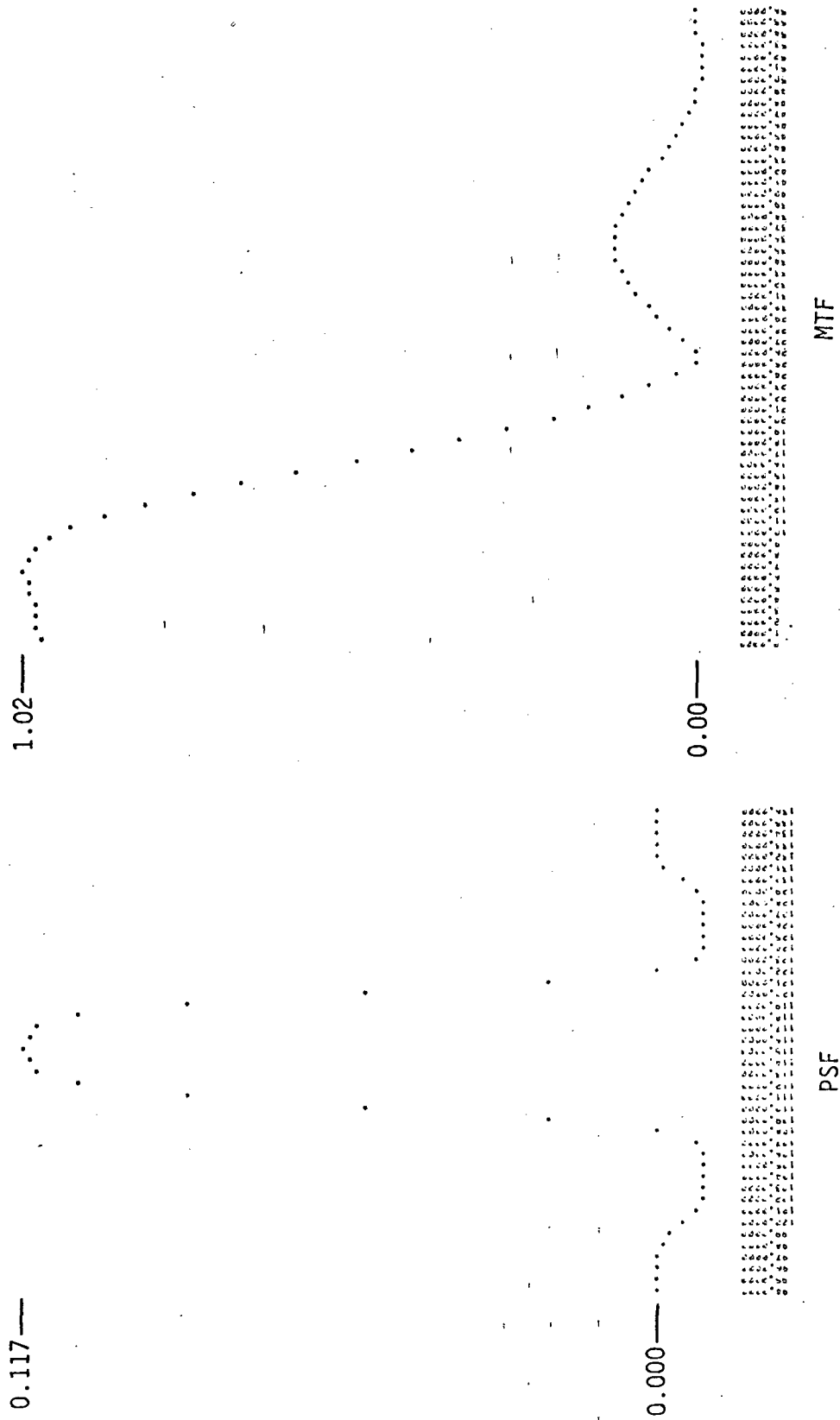


Figure 9 Along-Track PSF and its MTF Positioned on the Pixel  
 - S/N = 30, 40-Meter Sampling Interval

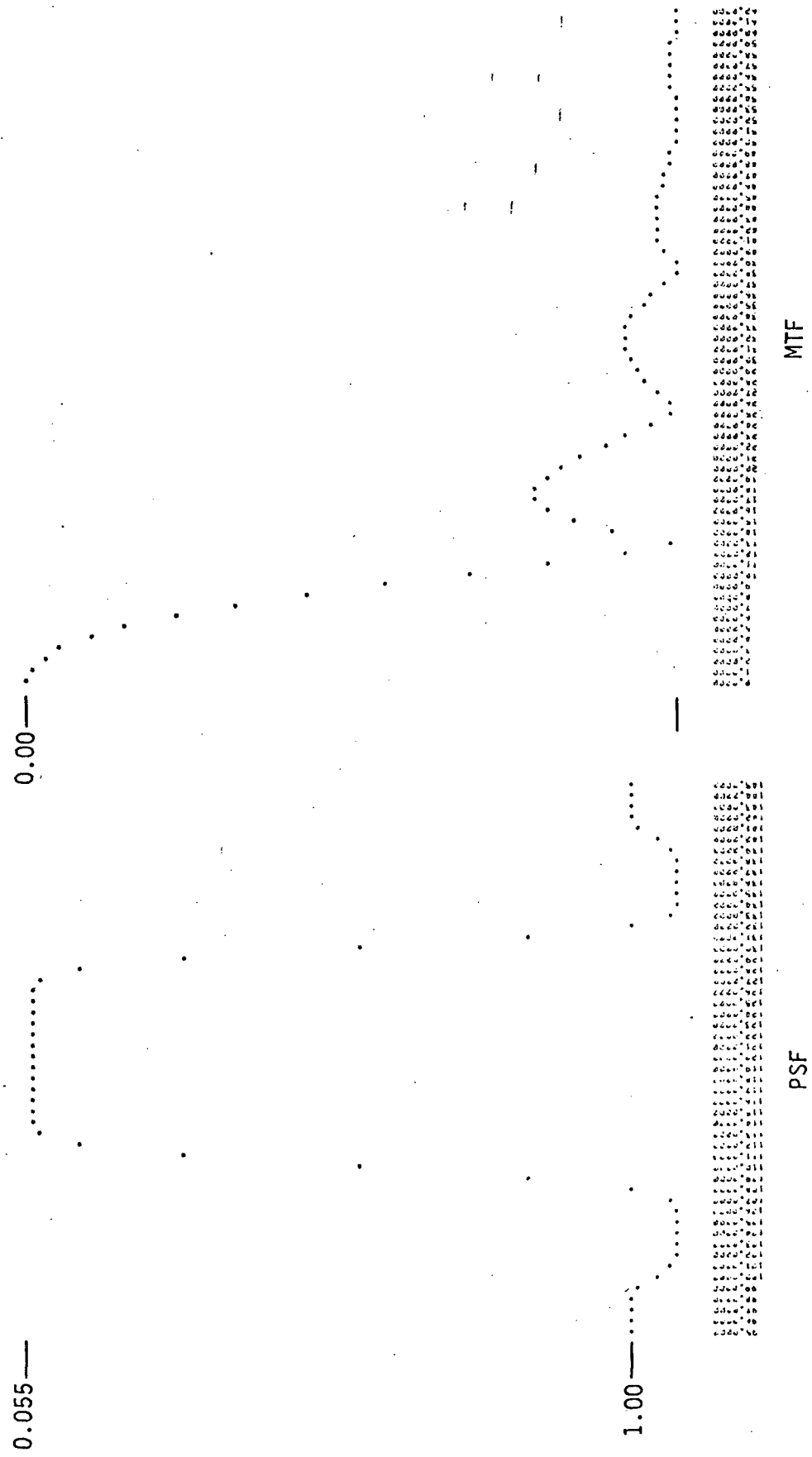


Figure 10 Along-Track PSF and its MTF Positioned Midway Between Pixels  
 - S/N = 30, 40-Meter Sampling Interval

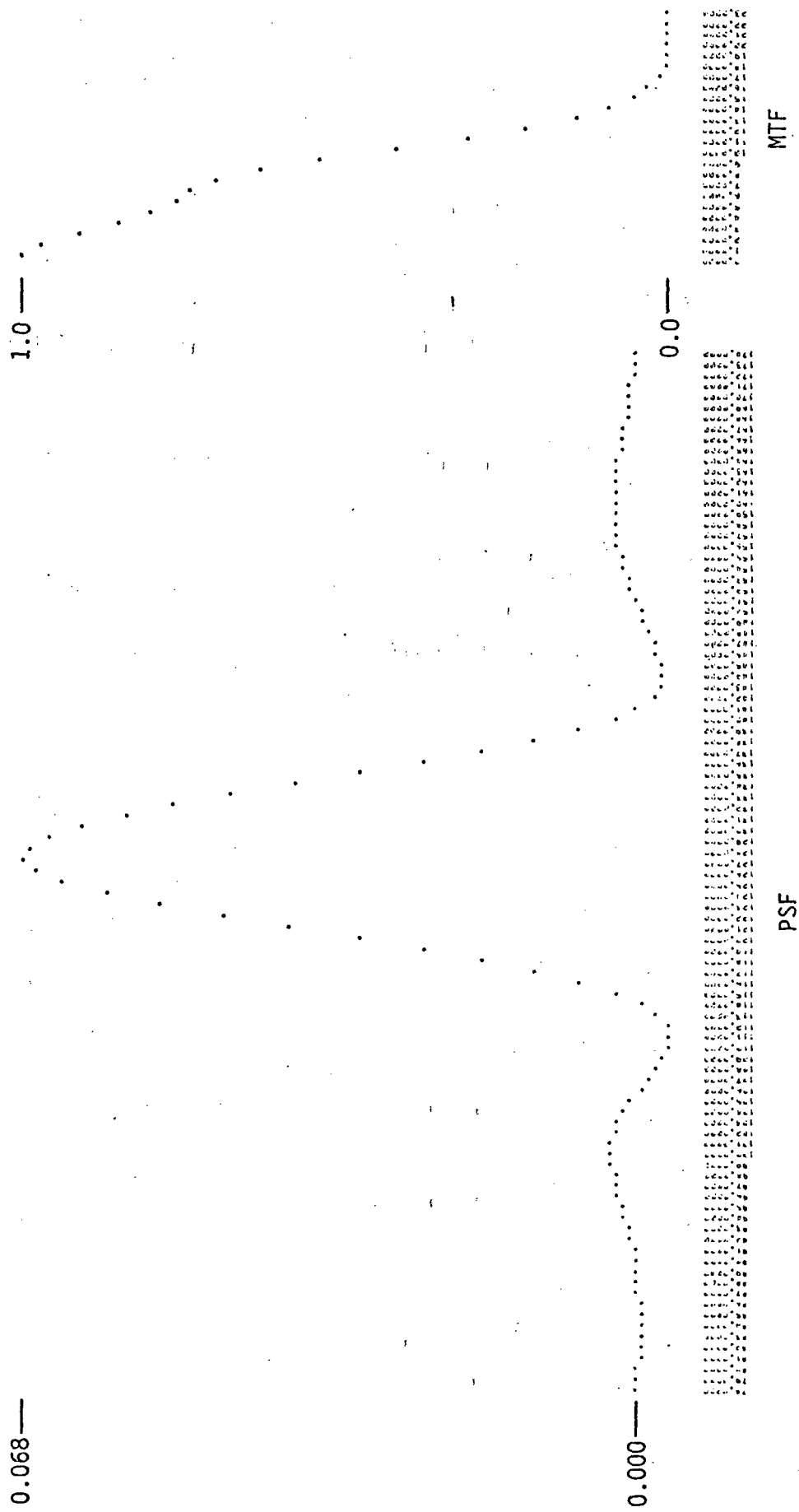


Figure 11 Across-Track PSF and its MTF Positioned on the Pixel  
 - S/N = 2, Original Sampling Interval

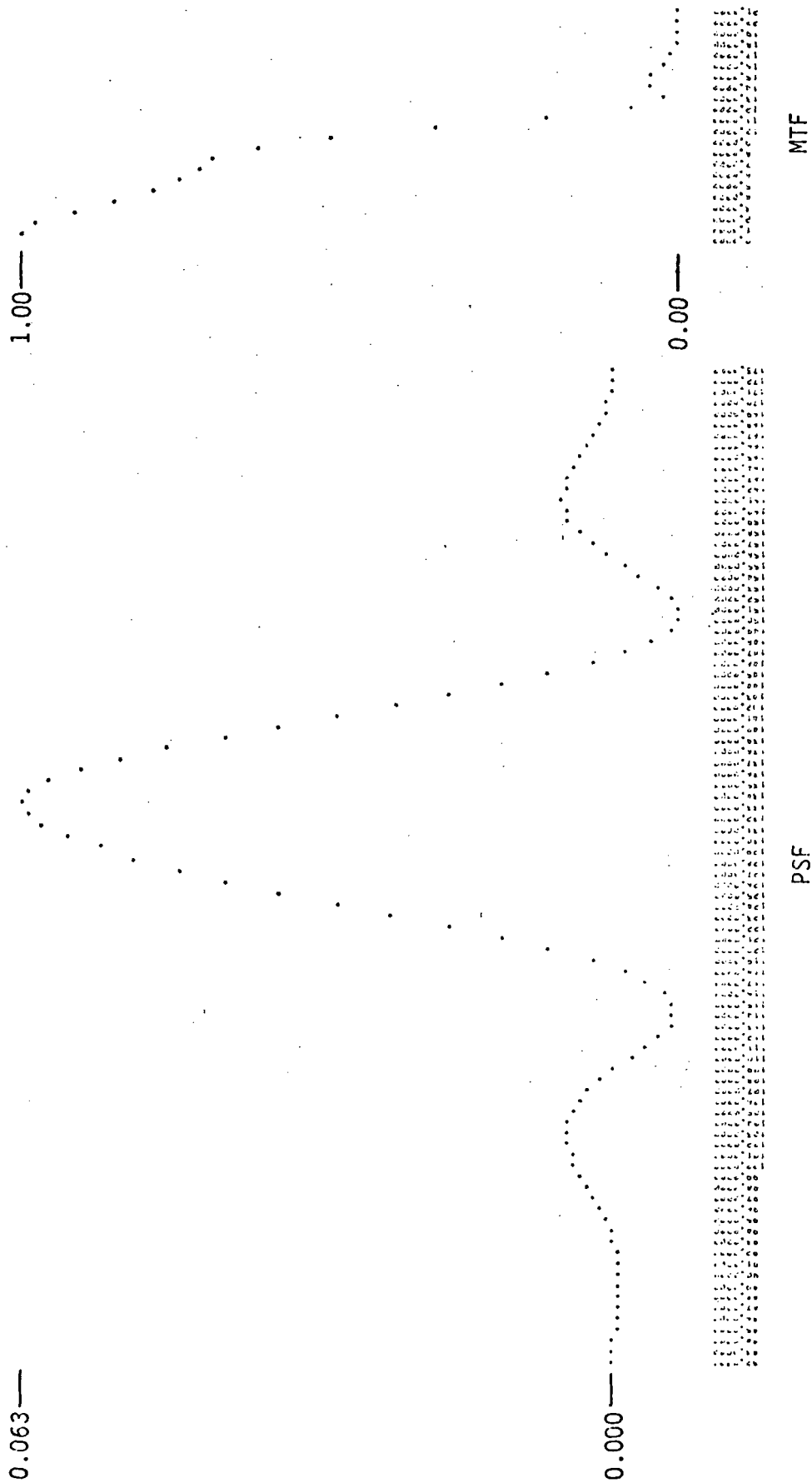


Figure 12 Across-Track PSF and its MTF Positioned Midway Between Pixels  
 - S/N = 2, Original Sampling Interval



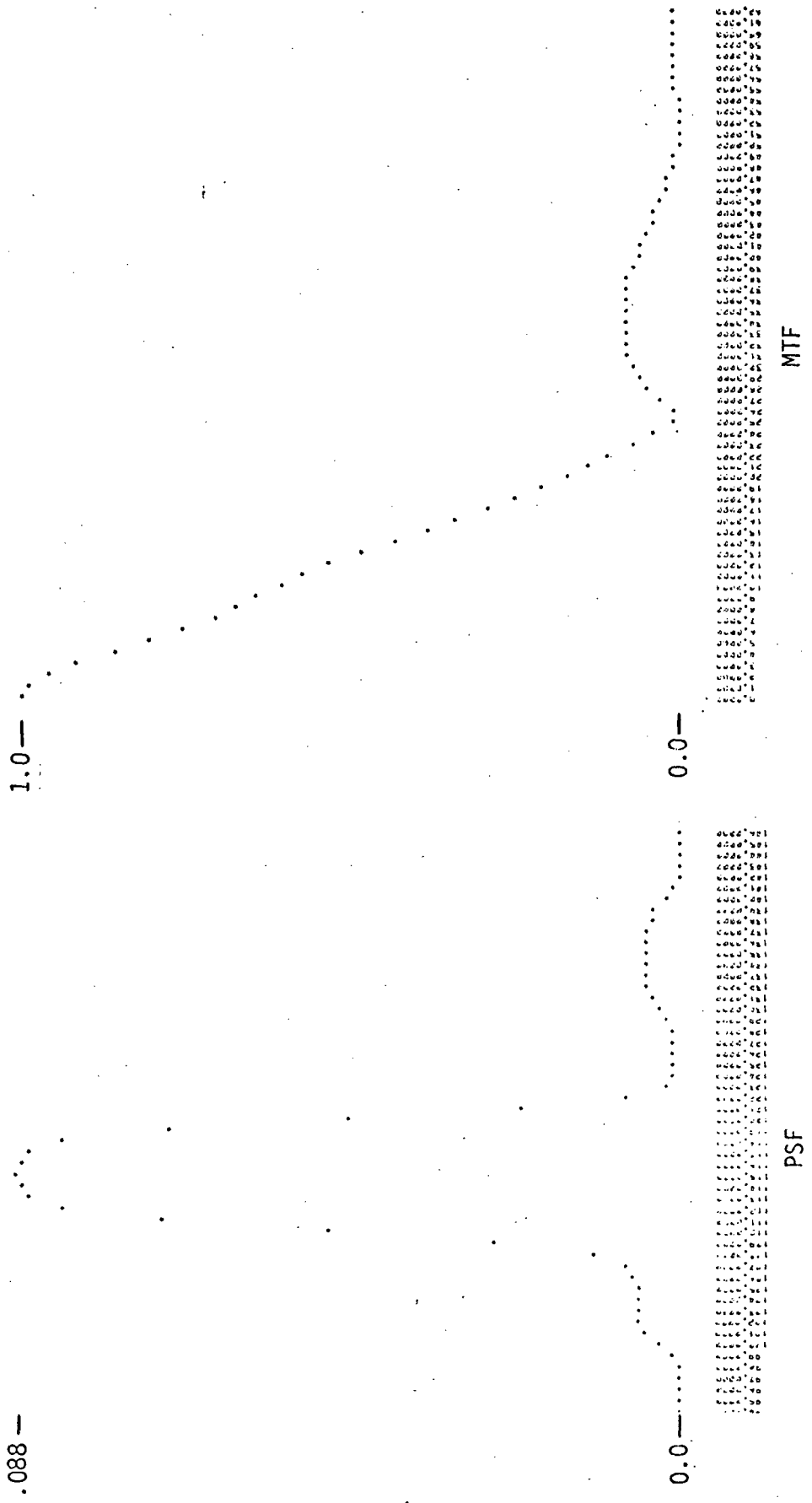


Figure 13 Along-Track PSF and its MTF Positioned on the Pixel  
 - S/N = 2, Original Sampling Interval

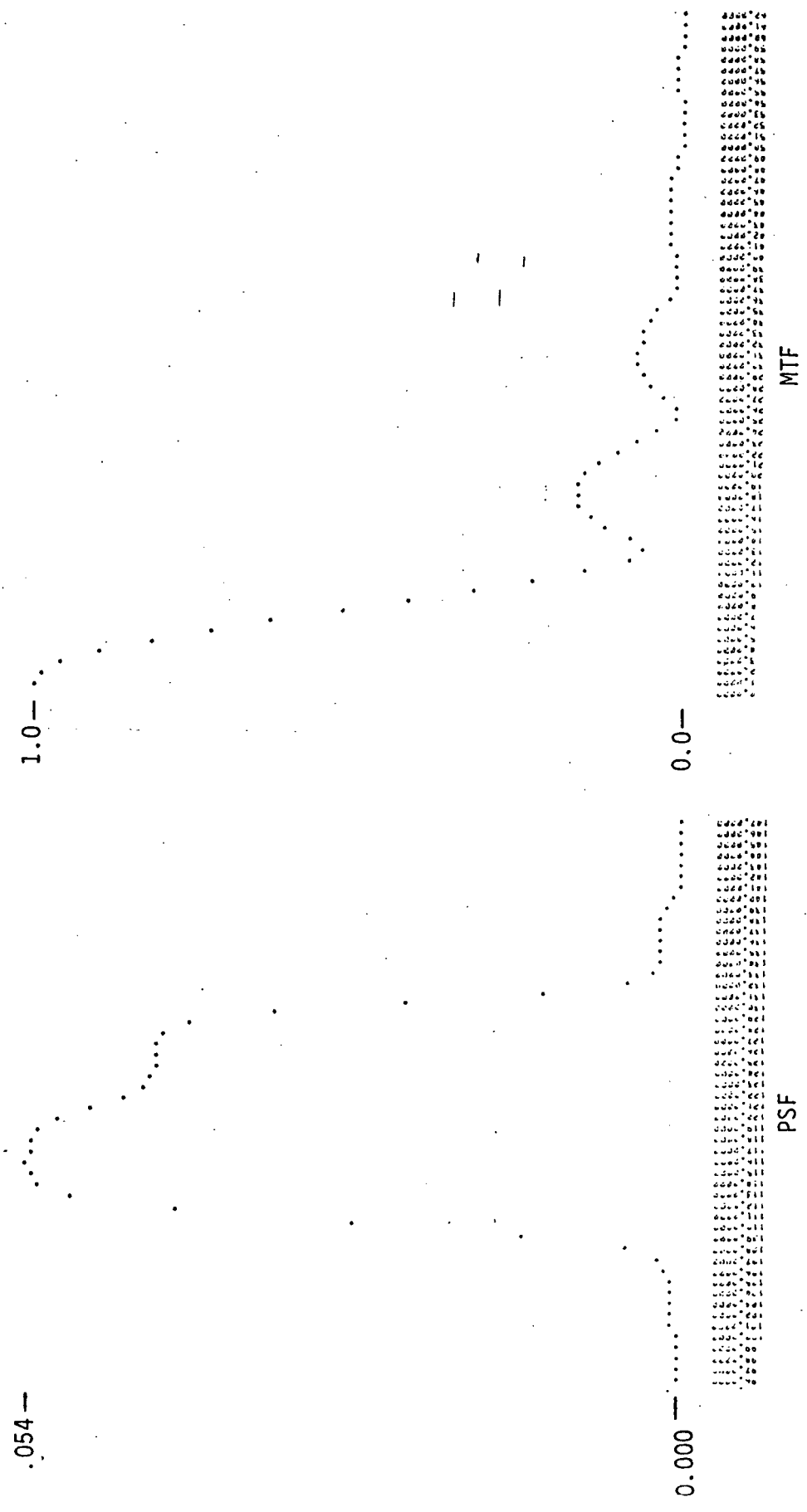


Figure 14 Along-Track PSF and its MTF Positioned Midway Between Pixels  
 - S/N = 2, Original Sampling Interval

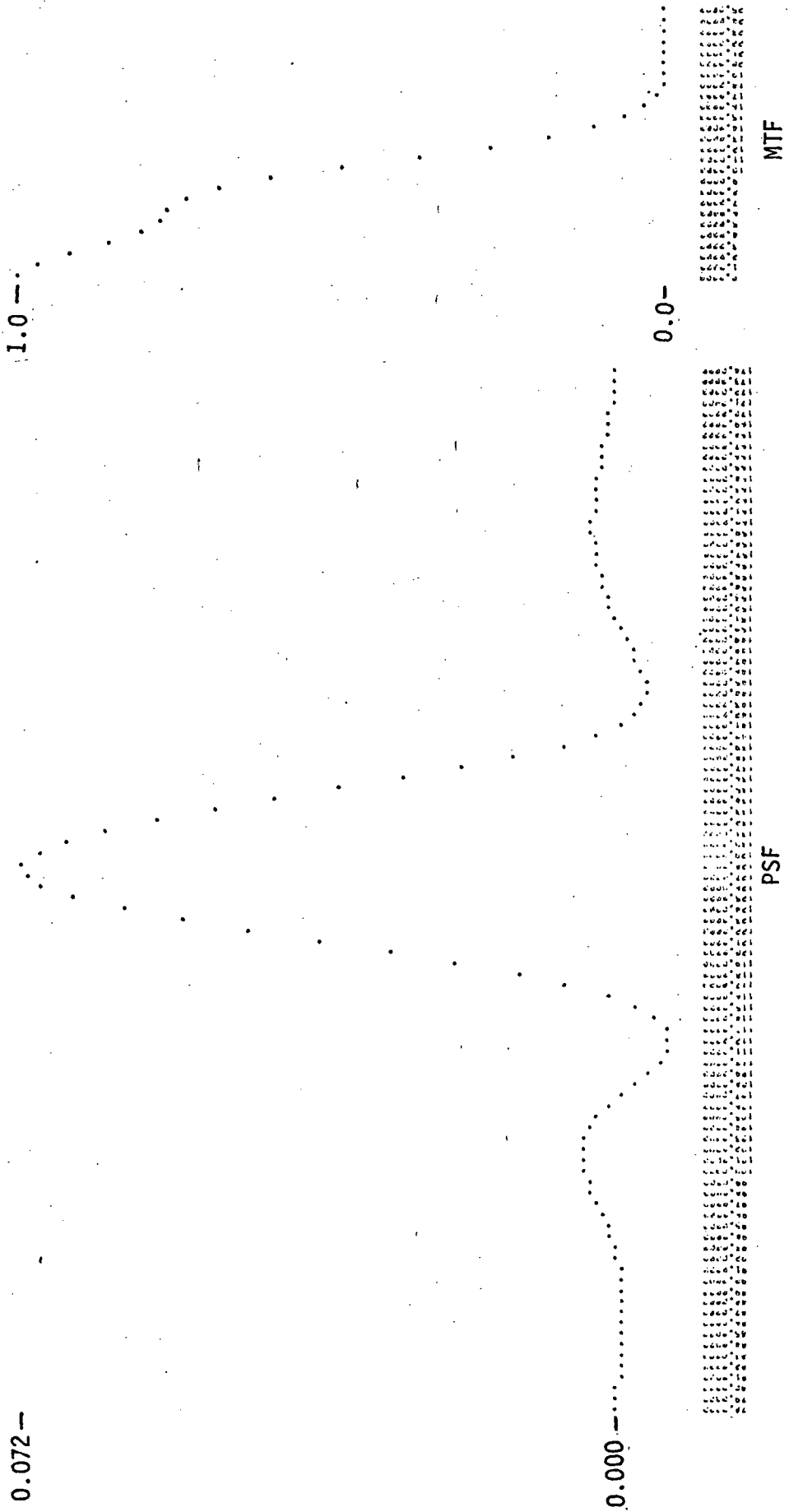


Figure 15 Across-Track PSF and its MTF Positioned on the Pixel  
 - S/N = 2, 40-Meter Sampling Interval

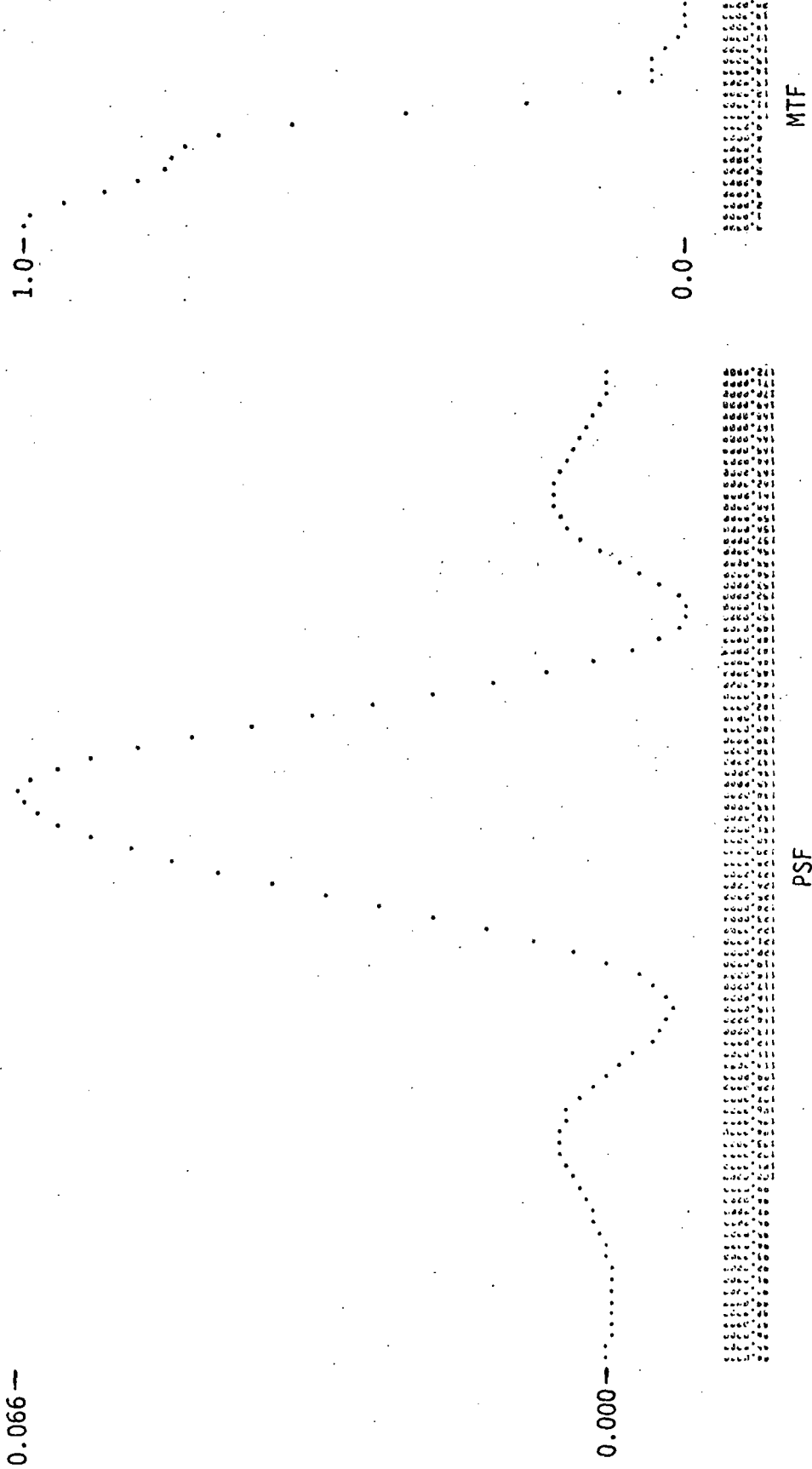


Figure 16 Across-Track PSF and its MTF Positioned Midway Between Pixels  
 - S/N = 2, 40-Meter Sampling Interval

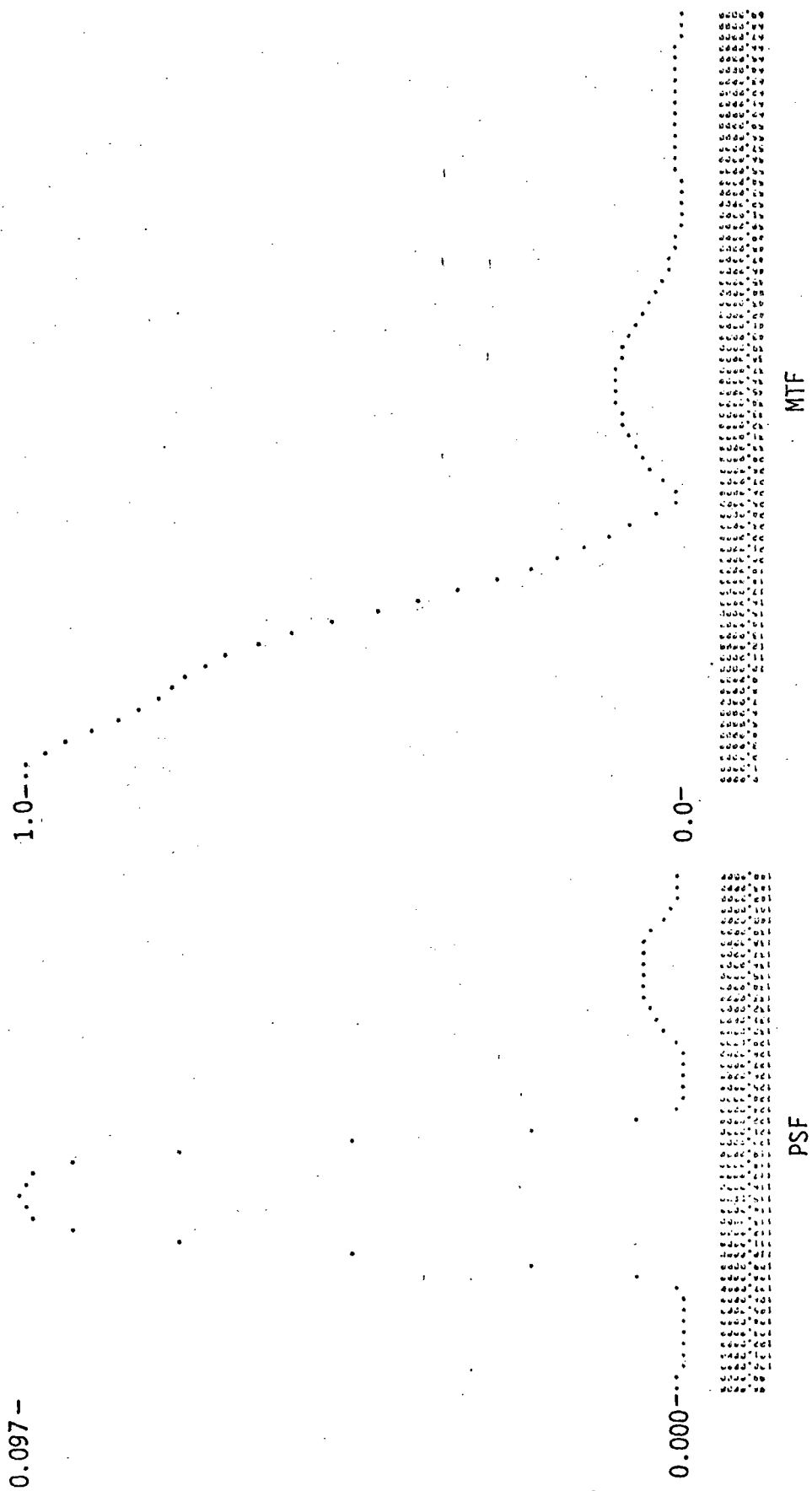
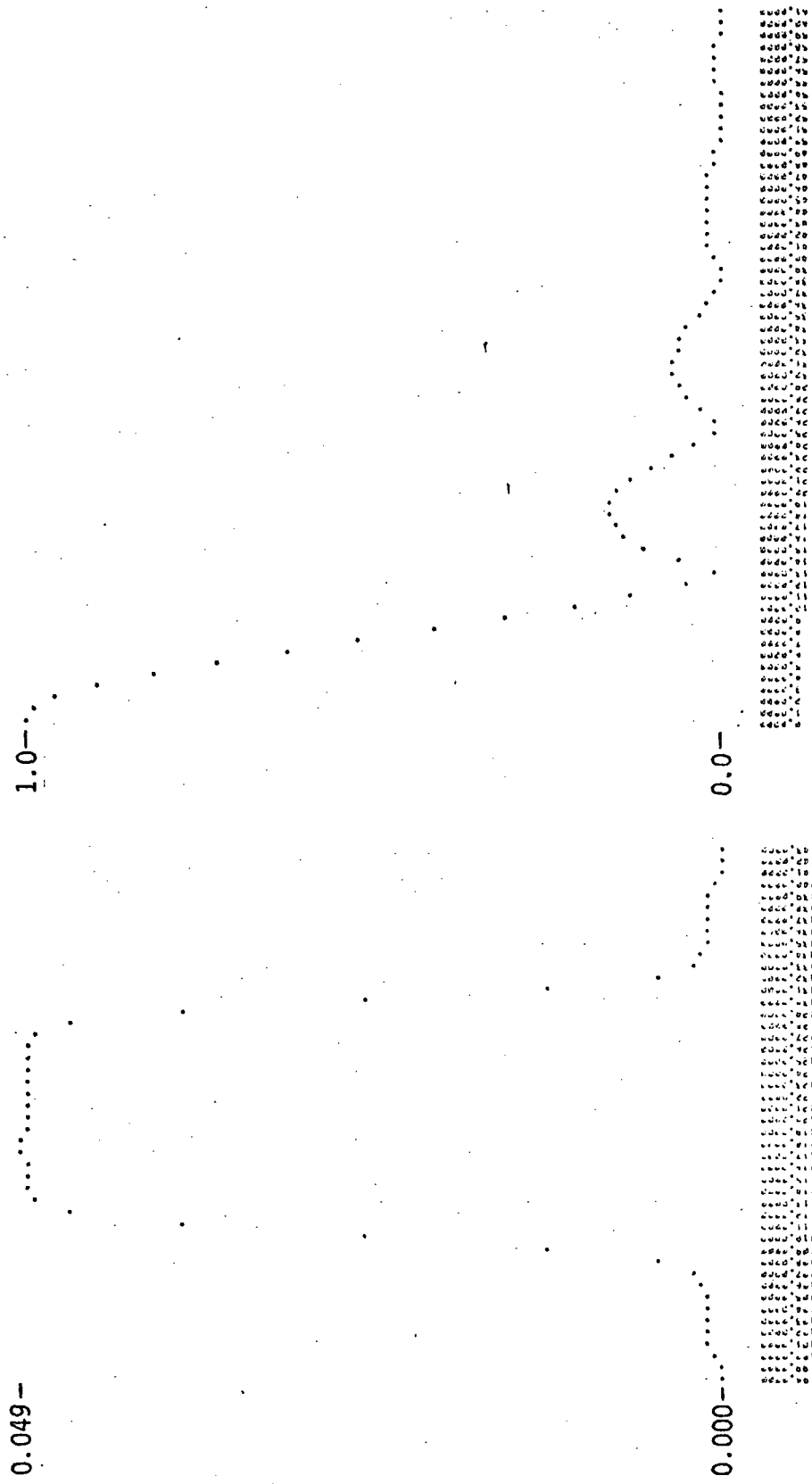


Figure 17 Along-Track PSF and its MTF, Positioned on the Pixel  
 - S/N = 2, 40-Meter Sampling Interval



MTF

PSF

Figure 18 Along-Track PSF and its MTF Positioned Midway Between Pixels  
 - S/N = 2, 40-Meter Sampling Interval

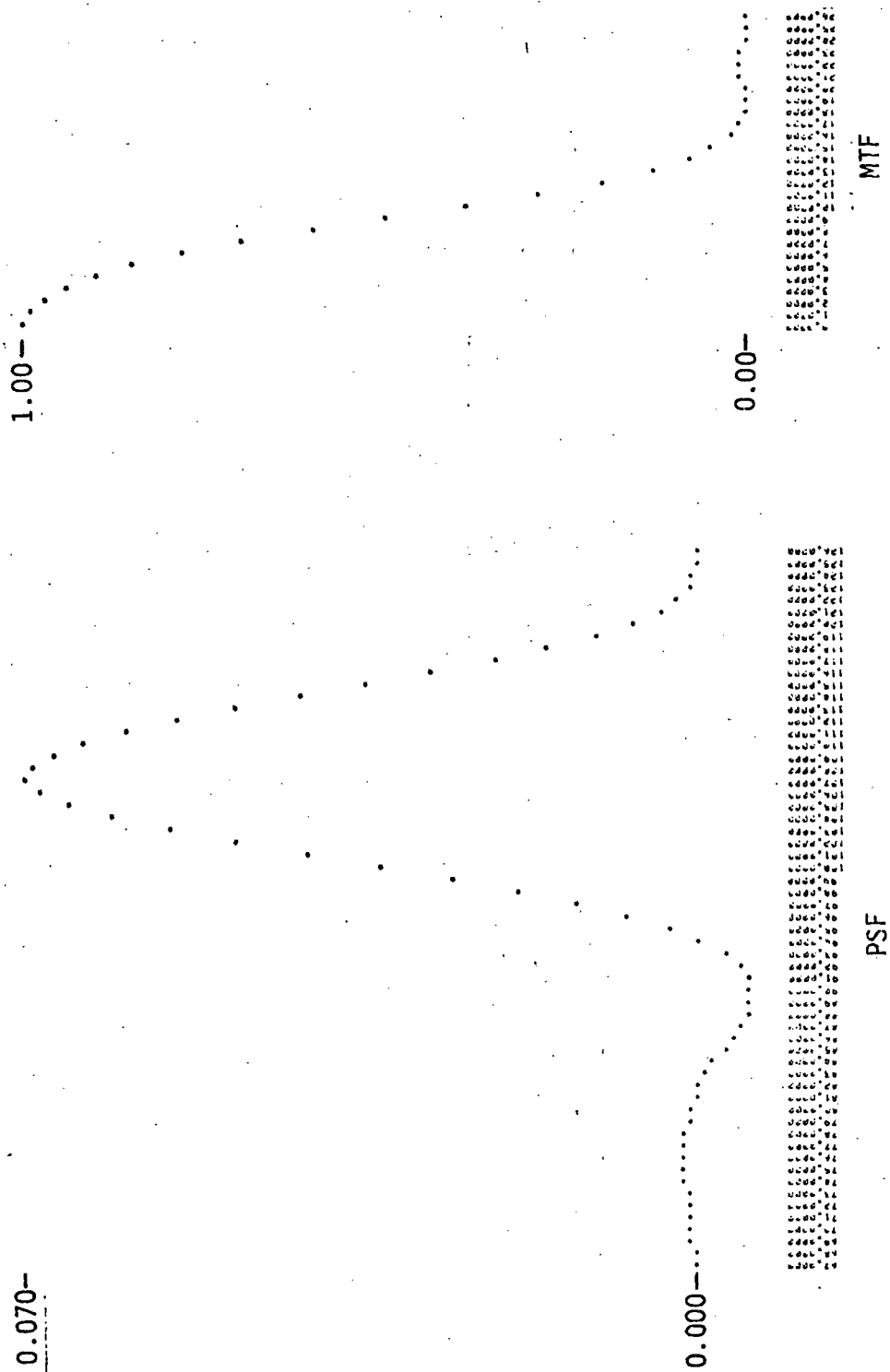


Figure 19 PSF and MTF for Cubic Convolution - Positioned on the Pixel, Original Sampling Interval

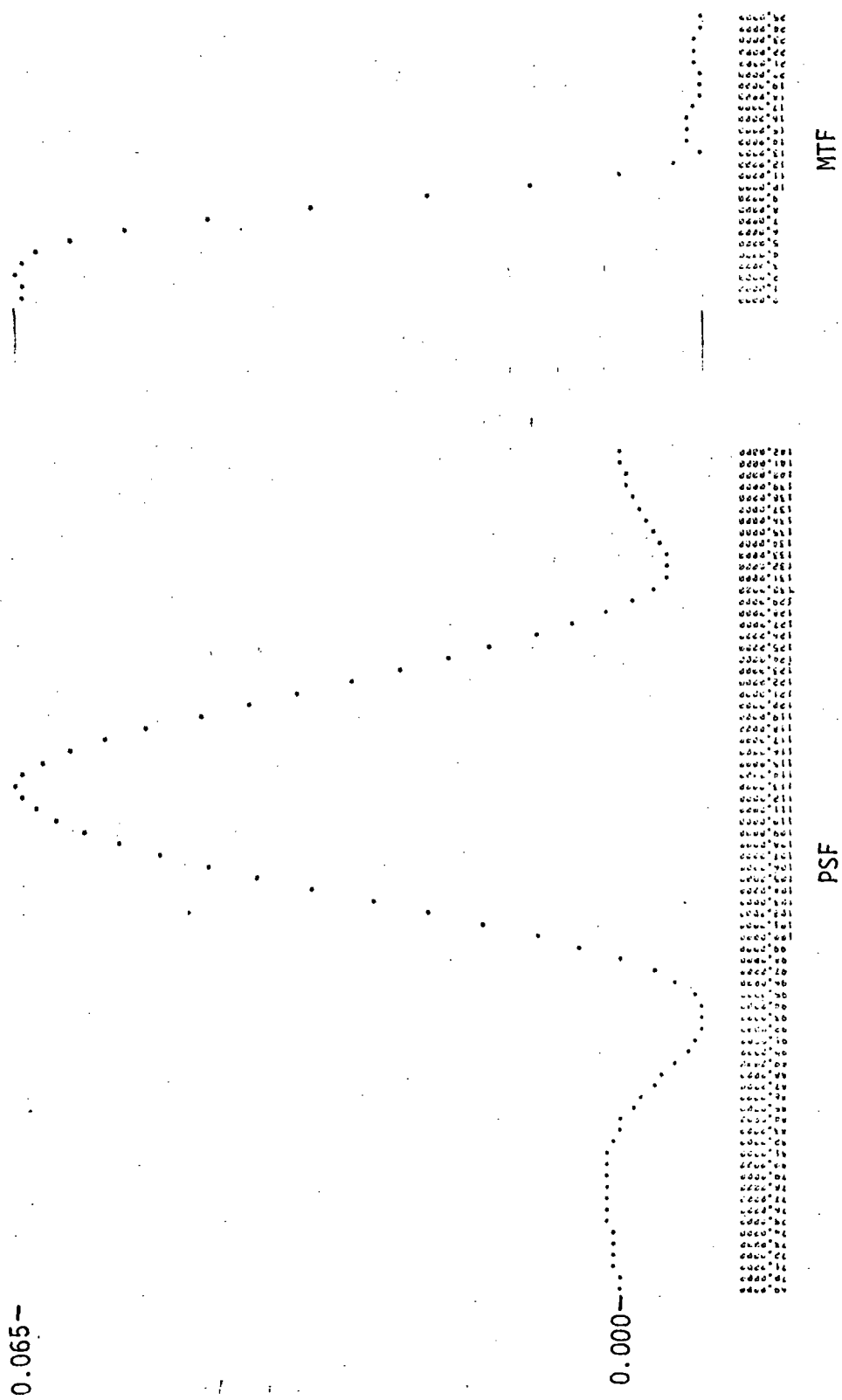


Figure 20 PSF and MTF for Cubic Convolution - Positioned Midway Between Pixels,  
Original Sampling Interval



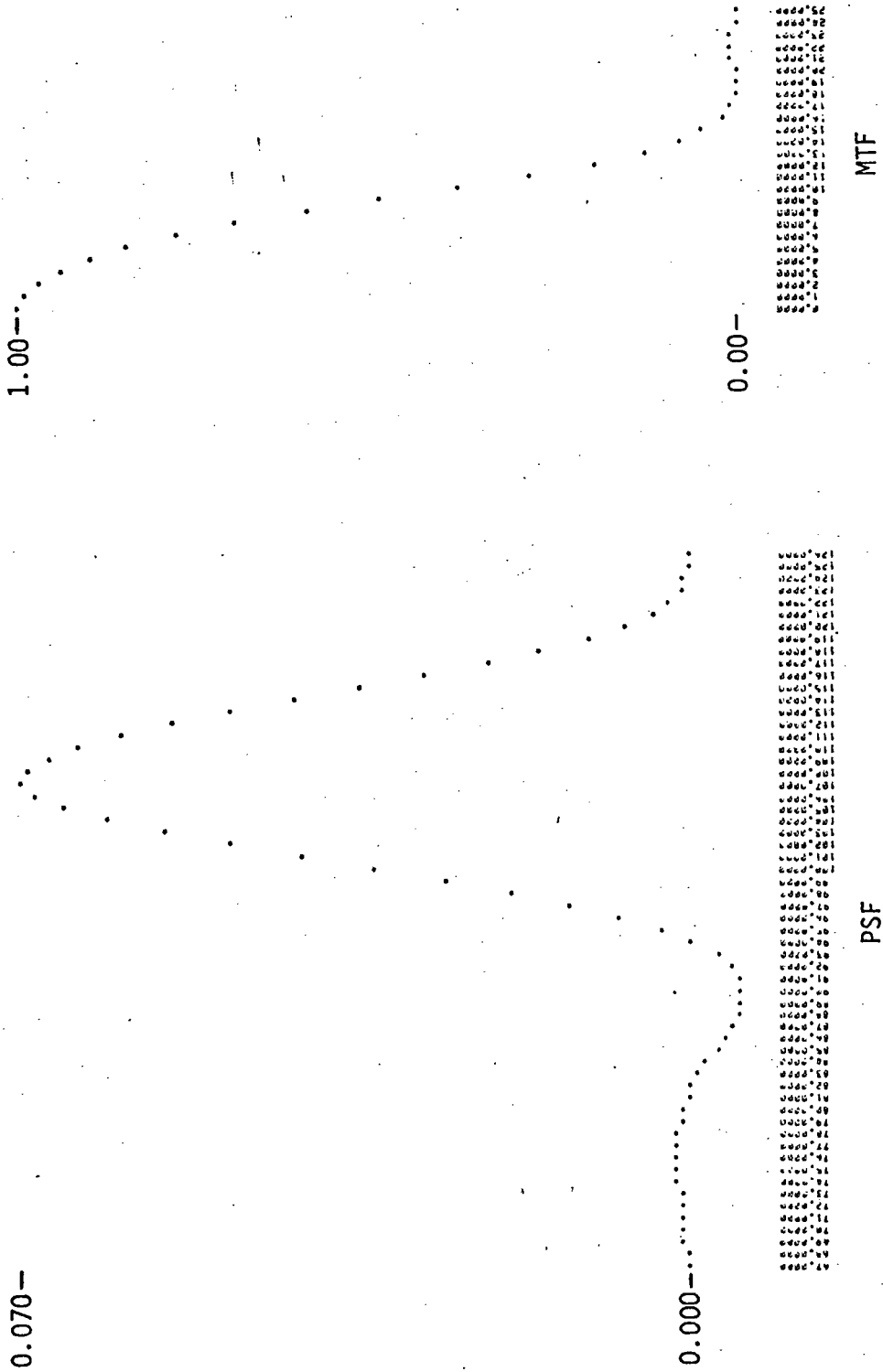


Figure 21 PSF and MTF for Cubic Convolution - Positioned on the Pixel,  
40-Meter Sampling Interval

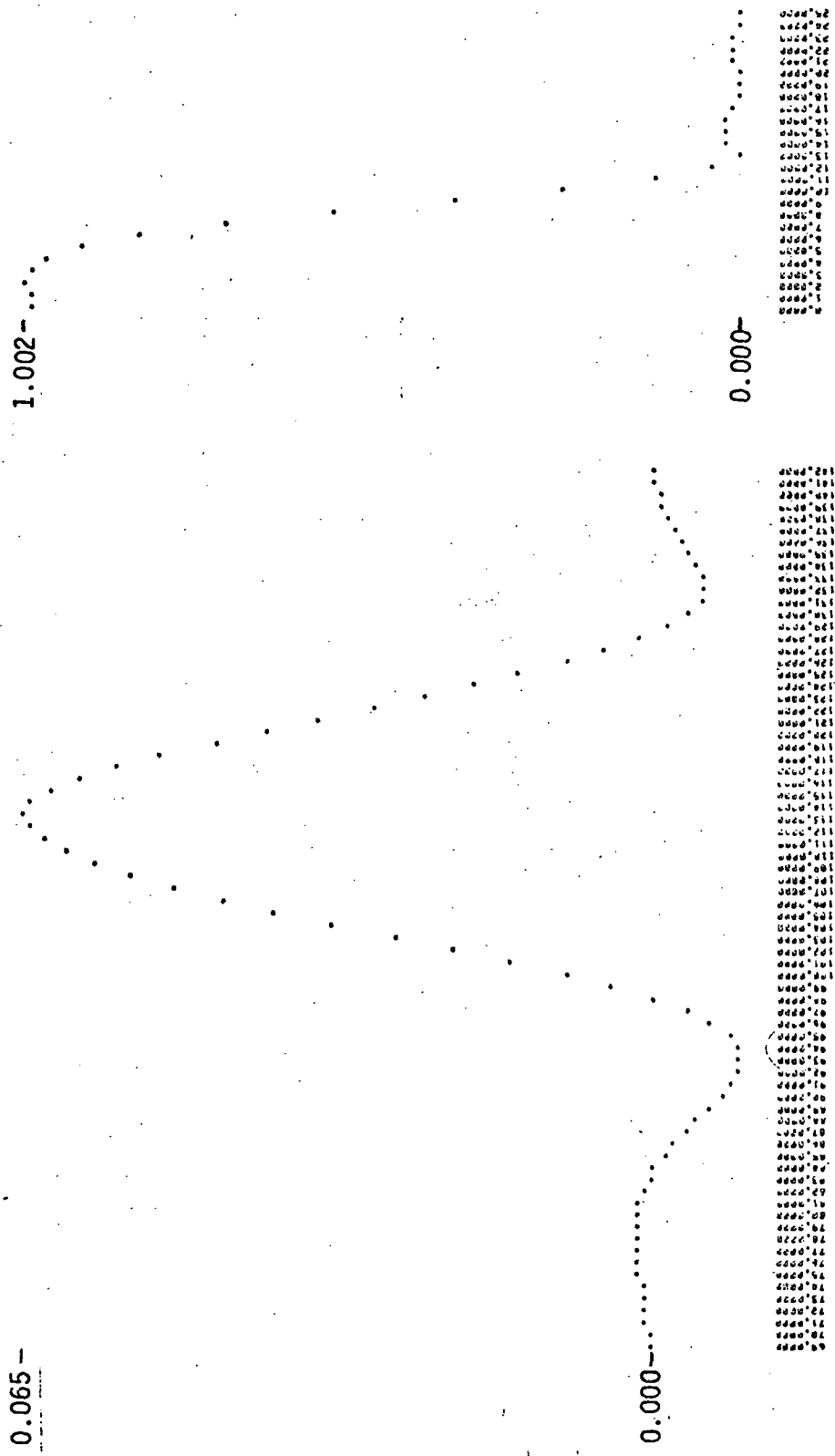


Figure 22 PSF and MTF for Cubic Convolution - Positioned Midway Between Pixels, 40-Meter Sampling Interval

## APPENDIX B

### REFERENCES

1. NASA Application Notice AN-OA-76-B
2. Colvo-coresses, Alden P. "Space Oblique Mercator", Photogrammetric Engineering, 1974, pp. 921-926.
3. Dye, Robert H. et al., "Quantitative Measurements of Air Pollutants by Long-Path Infrared Spectroradiometer," Seventh International Symposium on Remote Sensing of Environment, The University of Michigan, 1971.
4. Dye, Robert H. "Restoration of LANDSAT Images by Two Dimensional Deconvolution," Proceedings of the Tenth International Symposium on Remote Sensing of Environment. ERIM 6-10 October, 1975. pp. 725-730.
5. Rifman, Samuel S. " Digital Rectification of ERTS Multispectral Imagery," Proceedings of Symposium on Significant Results Obtained from ERTS-1, Greenbelt, Maryland, March 5-9, 1973 pp 1131.
6. Dye, Robert H., "Multivariate Categorical Analysis - Bendix Style," Bendix Report BSR 4149, June 1974.